Arqueología de la Arquitectura
23 January-December 2026, 464
ISSN-L: 0037-0894, eISSN: 1988-320X
https://doi.org/10.3989/arq.arqt.2026.464

STUDIES

From the quarry to the monument: integrated study of São João de Calvos Church (Guimarães, Portugal)

De la cantera al monumento: estudio integrado de la iglesia de São João de Calvos (Guimarães, Portugal)

Fabio Sitzia
Hercules Laboratory, University of Évora, Portugal
IN2PAST, Associate Laboratory for Research and Innovation in Heritage, Arts, Sustainability and Territory
Corresponding author: fsitzia@uevora.pt, https://orcid.org/0000-0002-4183-3370

Filipe Brandão
Escola de Arquitetura, Arte e Design (EAAD), University of Minho, Portugal
Lab2PT Laboratório de Paisagens, Património e Território
IN2PAST, Associate Laboratory for Research and Innovation in Heritage, Arts, Sustainability and Territory
filipe.brandao@eaad.uminho.pt, https://orcid.org/0000-0002-3378-0176

Paulo Bernardes
Archaeology Unit, University of Minho, Portugal
Lab2PT Laboratório de Paisagens, Património e Território
IN2PAST, Associate Laboratory for Research and Innovation in Heritage, Arts, Sustainability and Territory
pbernardes@uaum.uminho.pt, https://orcid.org/0000-0003-0838-1349

Vera Pires
DER and CERENA, Instituto Superior Técnico, University of Lisbon, Portugal
Hercules Laboratory, University of Évora, Portugal
IN2PAST, Associate Laboratory for Research and Innovation in Heritage, Arts, Sustainability and Territory
vera.pires@tecnico.ulisboa.pt, https://orcid.org/0000-0002-1457-1627

Rebeca Blanco-Rotea
Institute of Social Sciences, University of Minho, Portugal
Lab2PT Laboratório de Paisagens, Património e Território
IN2PAST, Associate Laboratory for Research and Innovation in Heritage, Arts, Sustainability and Territory
rebeca.branco.rotea@eaad.uminho.pt, https://orcid.org/0000-0003-3975-2149

Jorge Ribeiro
Institute of Social Sciences, University of Minho, Portugal
Lab2PT Laboratório de Paisagens, Património e Território
IN2PAST, Associate Laboratory for Research and Innovation in Heritage, Arts, Sustainability and Territory
jribeiro@ics.uminho.pt, https://orcid.org/0000-0002-1792-9145

Abstract: Romanesque churches are among the most significant elements of Portuguese heritage, due to their architectural and technical-constructive quality and the stonework. The regions of Minho and Douro have the highest concentration of examples. The use of Heritage Building Information Modelling (HBIM) tools now facilitates their protection, conservation, and promotion. This study presents the Romanesque church of S. João de Calvos (Guimarães, Portugal), which contains a wealth of architectural, historical, and technical-scientific information, recovered using different analysis tools applied to the study of its architecture and construction materials. A complete set of archaeological and physicochemical data on the materials was integrated into a Heritage Building Information Modelling model capable of managing geometric and non-geometric information. This is a pilot study for future initiatives, such as the "Route of the Romanesque" (*Rota do Românico*), incorporating the information into a municipal Heritage Building Information Modelling database for different purposes.

Keywords: building materials; stratigraphic analysis of walls; HBIM; geo-archaeology; *Rota do Românico*; medieval ecclesiastical architecture.

Resumen: Las iglesias románicas constituyen uno de los elementos más significativos del patrimonio portugués, por su calidad arquitectónica, técnico-constructiva, y el trabajo de cantería. Las regiones del Minho y el Duero concentran una mayor densidad de ejemplos. El uso de herramientas de Modelización de Información de Edificios Patrimoniales (Heritage Building Information Modelling, HBIM) favorecen hoy su protección, conservación y promoción. Se presenta el estudio de la iglesia románica de S. João de Calvos (Guimarães, Portugal), que contiene una gran cantidad de información arquitectónica, histórica y técnico-científica, recuperada mediante diferentes herramientas de análisis aplicadas al estudio de su arquitectura y materiales de construcción. Un conjunto completo de datos arqueológicos y físico-químicos de los materiales fueron integrados en un modelo HBIM capaz de gestionar información geométrica y no geométrica. Un estudio piloto para futuras iniciativas, como la "*Rota do Românico*", incorporando la información a una base de datos municipal Heritage Building Information Modelling con diferentes finalidades.

Palabras clave: materiales de construcción; análisis estratigráfico de paramentos; HBIM; geo-arqueología; *Rota do Românico*; arquitectura eclesiástica medieval.

Received: 01-10-2025 / **Accepted**: 18-05-2026 / **Published**: 28-07-2026

Citation: Sitzia, F., Brandão, F., Bernardes, P., Pires, V., Blanco-Rotea, R. and Ribeiro, J. (2026). "From the quarry to the monument: integrated study of São João de Calvos Church (Guimarães, Portugal)." *Arqueología de la Arquitectura,* 23: 464. DOI: https://doi.org/10.3989/arq.arqt.2026.464

Supplementary information ↓

1. INTRODUCTION

Romanesque architecture is not the product of a single nation, but rather a widespread European phenomenon that developed almost simultaneously across Italy, Spain, Germany, France, England, and Portugal. Throughout its evolution, it was shaped by complex exchanges and influences, contributing to a shared architectural culture across central-western Europe (Rudolph, 2019). Romanesque-style buildings, predominantly religious but also including military and, to a lesser extent, civil, represent a fundamental component of Europe's cultural heritage.

Today, the conservation, monitoring, and valorisation of this legacy, alongside traditional methods inherent to integrated heritage management, increasingly rely on advanced digital tools. Among these, Heritage Building Information Modelling (HBIM) has emerged as a key methodology over the past decade. The main reason is that it enables the creation of intelligent three-dimensional models that integrate not only geometric data, but also historical, archaeological, and technical-scientific information (Volk, Stengel, and Schultmann, 2014).

Unlike conventional Building Information Modelling (BIM), which is primarily used in contemporary construction and where the asset is built according to the model, Heritage Building Information Modelling is generated retrospectively from survey data, such as Unmanned Aerial Vehicle photogrammetry and laser scanning, and progressively enriched with additional datasets (Nguyen and Adhikari, 2023). Within the European context, BIM processes are regulated by the ISO 19650 standards, which have contributed to defining international and community frameworks for information management (Godager *et al.*, 2022; Pan *et al.*, 2024).

Both BIM and HBIM approaches rely on the integration of geometric and non-geometric datasets (Bastem and Cekmis, 2022; Borkowski and Kubrat, 2024; Charef *et al.*, 2019; Croce *et al.*, 2021; Wang and Kim, 2019).

These include: (i) historical, archaeological, and archaeometric data, which support analysis, research, education, and heritage dissemination; and (ii) documentation of the current condition of buildings and materials, primarily aimed at conservation professionals working in public administrations and heritage authorities. Considering the complexity of cultural heritage and the need for a common framework for collaboration between stakeholders, open Building Information Modelling practices reliant on Industry Foundation Classes (IFC), a standard vendor-neutral data schema defined in ISO 16739-1, are considered essential to allow data exchange and future reuse. The integration of datasets, such historical and archival documentation, as well as management and lifecycle data within Heritage Building Information Modelling applications has been explored by various authors (Chelaru *et al.*, 2024; Fitz and Saleeb, 2019; Lovell, Davies, and Hunt, 2023; Nieto-Julián *et al.*, 2025; Puerto *et al.*, 2024).

Heritage Building Information Modelling can support not only digital reconstruction and data standardisation, but also the analysis of building deterioration processes, including structural instability, material decay and performance (Coll-Pla *et al.*, 2019; Garagnani, Gaucci, and Gruška, 2016; Karasaka and Ulutas, 2023; Nieto-Julián *et al.*, 2025).

This study adopts an HBIM approach to perform an interdisciplinary, comprehensive analysis of a building included in the ‘Route of the Romanesque’ (*Rota do Românico*), a cultural itinerary comprising 58 monuments located in northern Portugal, along the *Sousa*, *Tâmega*, and *Douro* river valleys. This route includes churches, monasteries, bridges, castles, and towers, all characterised by Romanesque architecture. The sites are located within a geographical area defined by Porto, Guimarães, and the *Douro* Valley, all recognised as UNESCO World Heritage Sites.

The inclusion of these monuments as part of the route has not always been accompanied by an exhaustive study of the selected examples, at least not through more recent methodologies closely connected to the materiality of the building, nor through a cross-disciplinary approach. This may lead to misinterpretations, for instance, of their construction sequence, or to insufficient data, resulting in oversimplifications and, at times, the transmission of incomplete information to visitors.

The underlying objective of this work is therefore to develop a management model for this type of built heritage that is rigorous, interdisciplinary, integrated, and easy to use for professionals responsible for promoting, maintaining, and enhancing the entire route or for managing individual buildings. At the same time, it should be simple, so that it can be effectively implemented by professionals without extensive technical expertise, which would otherwise require specialized training not always feasible within small municipal administrations.

The case study focuses on the Romanesque-style Church of São João de Calvos (Guimarães, 13th century AD).

The proposed integrated model combines Heritage Building Information Modelling with archaeometric and archaeological stratigraphic analysis. This latter process is based on the identification of stratigraphic units (SU), defined as individual constructive or destructive actions preserved within the structure.

Each unit reflects either human or natural processes and can be grouped into distinct phases. The reconstruction of their spatial and temporal relationships enables a detailed interpretation of the building's construction history.

In addition, through Heritage Building Information Modelling, this study includes the identification of the types of building materials, as a necessary preliminary phase for future research aimed at determining the quarries from which the construction stones were extracted. Likewise, a series of pathologies have been identified, resulting either from the building's own constructional evolution or from its abandonment until the reconstruction of the roof in the second half of the 20th century.

The case study of São João de Calvos highlights how the monuments included in the 'Route of the Romanesque' often extend beyond a strictly Romanesque phase, revealing more complex construction histories that require accurate documentation and interpretation.

Within this framework, the paper discusses the integration of semantic data into HBIM models, including historical, archaeological, and restoration-related information. Attention is given to the representation of construction materials through thematic mapping techniques. These include ultrasonic pulse velocity (UPV) surveys and geological analyses, which are used to assess the conservation state of the building (Casula *et al.*, 2026; Fais *et al.*, 2017; Hatır, Korkanç, and Başar, 2019; Pucci, 2014; Stück, Siegesmund, and Rüdrich, 2011). These datasets are implemented as interactive layers within the 3D model, allowing for advanced visualisation and analysis.

Furthermore, laboratory analyses using different diagnostic techniques have been carried out to identify the physicochemical features of building materials. This information is essential for supporting restoration interventions, particularly in selecting compatible materials for the replacement of deteriorated stone elements (Colao *et al.*, 2010; Columbu *et al.*, 2022).

2. RESEARCH BACKGROUND

Existing approaches to integrating stratigraphic information into Heritage Building Information Modelling models typically rely on geometric-driven segmentation, frequently handled by explicitly 3D modelling (Brusaporci *et al.*, 2018; Mammoli, Mariotti, and Quattrini, 2021; Santoni *et al.*, 2021). While this strategy enables the generation of phased models and hypothetical reconstructions of heritage assets, it is inherently time-consuming and demands advanced expertise in both geometric modelling (e.g., Non-Uniform Rational B-Splines NURBS-based workflows) and Building Information Modelling authoring. More critically, it assumes that the semantic structure of the building can be adequately represented through a predefined geometric subdivision.

Alternative strategies explored semantic enrichment at earlier stages of the workflow using machine learning techniques to classify point clouds, associating semantic information directly with survey data (Croce *et al.*, 2021). However, this approach operates at the level of data preprocessing and does not address how heterogeneous and potentially non-aligned analytical layers can be managed within a Heritage Building Information Modelling environment.

In an earlier approach, Chiabrando, Lo Turco, and Rinaudo (2017) introduce two-dimensional surfaces to document material decay, thereby circumventing the need for geometric subdivision, yet these seem to remain external or auxiliary to the HBIM model. Although their approach focused only on material damage, it is highly relevant to the current study. They use image textures as a repository of semantic information at low Level of Detail (LoD), which constitutes a flexible approach for ongoing studies. They also present work on two more levels of detail, subdividing walls into brick elements, although highlighting the non-standard nature of the resulting IFC models. A similar approach for integrating non-destructive testing results into Heritage Building Information Modelling was explored by (Solla *et al.*, 2020) with JPEG images attached to virtual surfaces overlayed on wall objects in Revit. Yet, the application specific approach prevented exporting the data to IFC.

The assumption of a predefined geometric subdivision becomes problematic when multiple analytical layers are considered simultaneously, as in this study. Stratigraphic units, material classifications, and degradation patterns often define spatial partitions that are non-coincident and originate from different disciplinary perspectives. Representing these overlapping and heterogeneous interpretations through geometric subdivision leads to a rapid increase in model complexity. Each additional layer of analysis potentially requires further segmentation of the model, resulting in a combinatorial expansion of elements.

An apparently straightforward solution is to adopt the smallest possible unit of subdivision, such as the individual stone block. However, this approach does not resolve the issue. Different analytical frameworks may still require finer or alternative partitions that do not align with the chosen geometric discretization (e.g. weathering gradients or mineral heterogeneity). More fundamentally, there is no stable or universal minimum unit of analysis across disciplines. As a result, the model becomes both increasingly complex and structurally inadequate to accommodate evolving knowledge.

Moreover, this geometry-driven approach necessitates an *"a priori"* coordination between stakeholders to define a shared subdivision logic before modelling begins. Such a requirement introduces a rigid and synchronous workflow, which is at odds with the iterative and cumulative nature of heritage documentation, where new data and interpretations emerge over time.

To address these limitations, this study proposes an alternative approach based on the decoupling of semantic information from geometric subdivision. Instead of encoding analytical results through the fragmentation of the 3D model, information is represented using two-dimensional masks that are mapped onto the surface of a simplified geometric model. In this framework, the three-dimensional model acts as a stable spatial support, while analytical layers—such as stratigraphy, material characterisation, or degradation—are independently defined and overlaid as surface-based representations.

This approach is more closely aligned with how data is produced in heritage studies, where analyses are typically conducted through drawings, maps, or image-based annotations. By preserving this logic, stakeholders can contribute using their own domain-specific tools without requiring expertise in 3D modelling. At the same time, the model remains open to incremental updates, as new analytical layers can be incorporated without modifying the underlying geometry.

Ultimately, this shift from geometry-driven segmentation to surface-based semantic layering enables a more flexible, scalable, and epistemologically consistent integration of heterogeneous datasets within an HBIM environment. The contribution of this study is therefore not the introduction of semantic information into HBIM per se, which is already established in the literature, but rather the proposal of a lightweight IFC-compatible strategy for managing heterogeneous and non-coincident analytical layers without requiring geometric subdivision of the architectural model.

3. THE ROMANESQUE-CHURCH OF S. JOÃO DE CALVOS

The church of S. João de Calvos (geographical coordinates: 41° 22’ 29.74” N, 8° 21’ 53.06” W, Fig. 1), has been classified as a Property of Public Interest since 1955. It currently belongs to the parish of Lordelo, a situation already documented in the mid-16th century (Pina, 1952). It originally served an old parish, already mentioned in the 1220 inquiries of King Afonso II, and referred to as *Sancto Johanne de Calvos*, in the land of *Vermuy*, which disappeared during the Middle Ages.[1]

Additionally, there are other references to the parish in various documents from the 12th and 13th centuries, notably in a deed of exchange dated 1172 referring to the *vila Calvos*; in a sales contract dated 1246, referred to as Pactum venditionis fundi in Sancto Johanne de Calvos; and in the 1290, 1301, and 1308 inquiries of King Dinis. Concerning the structure itself, it is recorded in the inquiries of King Afonso III as Ecclesie Sancti Johannis de Calvis. Later, it is mentioned again in the Memórias

[1] https://servicos.dgpc.gov.pt/pesquisapatrimonioimovel/detalhes.php?code=73726

Paroquiais of 1758 (Cardoso), in the inquiry concerning Lordelo, in which the parish priest reports on the chapel of São João de Calvos, situated in the place of the same name, noting that it was not the destination of any pilgrimage. Very little additional information about the building is provided in either primary or secondary sources, with only brief references to its existence and a few limited studies of its architecture, generally defined as Romanesque in style.

The church preserves some elements of the original construction, but the nave and the apse are from different periods. Several construction phases are visible, resulting from changes made over time, particularly during the modern era. In several locations, negative imprints reveal the remains of structures that have since disappeared, notably those associated with the main and side doors, or with a high choir once located inside the church. The altarpieces installed in the 18th century were removed and taken to a private residence in the 1950s (De Pina, 1952). Left in a state of ruin during the 20th century, with its interior completely exposed, the church was restored by the *Direcção Geral dos Edifícios e Monumentos Nacionais* in the 1970s.[2]

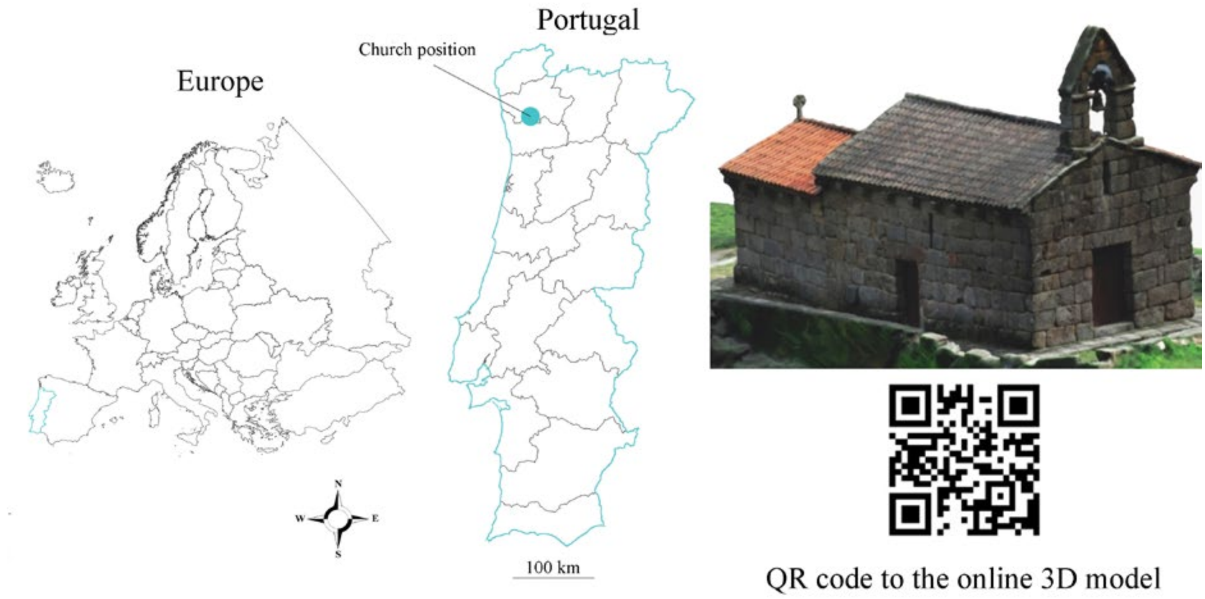

Figure 1. Geographic location and online-consultable 3D model of the church of S. João de Calvos (12th/13th century AD). Digital processing by authors.

S. João de Calvos is clearly an example of late rural Romanesque architecture from the 12th/13th centuries: modest, solid, and artistically simple. However, as we shall see, the analysis of masonries has revealed a greater complexity than was initially thought, according to the historiographical studies carried out to date. Small in size, it has a longitudinal plan consisting of two juxtaposed rectangular volumes: the nave and the apse. The main façade, south-west facing, ends in a gable topped by a bell tower also finished with a gable. The walls are made of granitoid roughly-hewn ashlars, horizontally arranged, with a somewhat rough cut, and displaying varying colours and textures. Many of the elements are heavily eroded, and some visible damage can also be observed.

The interior benefits from limited natural lighting, provided by seven openings: three doors and four narrow slit windows (one on each façade). In the mid-20th century, the interior was lime-coated (Pina, 1952), and traces of wall paintings are still visible today. On the walls, at mid-height and engraved into the masonry with traces of red paint, several Maltese crosses inscribed within circles have been preserved, corresponding to various stations of a *Via Crucis*.

2 https://atlas.cm-Guimarães.pt/pt/projeto/equipa

Also noteworthy are the corbels on the side façades, supporting a simple cornice formed by 16 elements, 10 on the north-western and south-eastern walls of the church's nave, simple in design, and another 6 on the walls of the apse, more elaborate and differing from one side to the other. All the corbels are in cavetto style, but some on the apse feature small geometric decorations, such as a sphere.

4. MATERIALS AND METHODS

4.1. Identification of stratigraphic units: the stratigraphic analysis of the building's walls

An essential part of the study conducted was the identification of the church's construction sequence to determine which preserved elements belong to the original phase and which represent later transformations, including their chronology and decorative characteristics. To achieve this, we applied one of the main methodologies of the archaeological discipline known as Archaeology of Architecture (Azkarate, 2013; Azkarate, Caballero and Quirós, 2002; Blanco-Rotea, 2017) specifically the reading of elevations or stratigraphic analysis of façades (Caballero, 1995). This discipline aims to explain past societies from a spatial perspective, through their immovable material culture, using archaeological methods in collaboration with other fields such as architecture, geospatial technologies, art history, and documentary history.

The reading of elevations consists of identifying the construction sequence by adapting the archaeological excavation and recording method known as the Harris Matrix (Harris, 1989) to the study of historical buildings. These are understood as stratified entities, in which construction and destruction actions are seen as stratigraphic units (SU) that accumulate over time within the structure.

The method involves identifying, georeferencing on the building's elevations, recording, and subsequently organizing the construction and destruction actions into the building's stratigraphic sequence, which represents the chronological order of these actions. For example, the nave wall would be a stratigraphic unit of the constructive element type (SU012); a window opened later would be a stratigraphic unit of the interface type (SU065) that cuts into the wall (SU012); and the infilling of the window opening (SU070) would be a new SU of the element type. In this sequence, wall SU012 is cut by interface SU065, and SU070 fills the cut made by SU012.

Once units are identified, plotted on the plans, and described, recording their physical relationships (cuts, joins, abuts, covers, fills) and temporal relative chronology, they are organized into a stratigraphic diagram (Harris Matrix). Here the oldest elements are at the bottom and the most recent at the top. Thanks to the final stages within the stratigraphic analysis of elevations—synthesis, correlation, and periodization—stratigraphic units (SU) with the same function and chronology are grouped into Activities (A), and these in turn into construction phases. The application of this methodology has made it possible to identify three construction phases in São João de Calvos, each with their corresponding sub-phases. This information was subsequently incorporated as images into the Heritage Building Information Modelling with the aim of making the sequence understandable within the geometry of the monument.

4.2. Building materials analysis

To perform physical and mineralogical analyses, stone materials were sampled from the closest outcrops exhibiting lithologies comparable to those of the monument.

Petrographic characterisation was done by thin sections observation according to the standard UNI EN 12407:2007 (Natural stone test methods – Petrographic examination). Physical characterisation was done following the recommendations of UNI EN 1936:2001 (Natural stone test method – Determination of real density, apparent density, total and open porosity).

On the building, the ultrasonic pulse velocity was measured by a Proceq PL200 pundit and 54 kHz exponential transducers. For each ashlar, the ultrasonic velocity was recorded at five distinct points (10 cm offset). The resulting data were averaged to determine the mean velocity for each block.

By using these values, the Velocity Ratio Index (VRI, Equation [1]) was calculated:

$$VRI = (V_{pf}/V_{pi})^{0.5} \quad \text{[equation 1]}$$

This index allowed for the measurement of the quality of building materials proposed by Kahraman, Ulker, and Delibalta (2007), which is also adopted by other researchers in the application of non-destructive integrated techniques (Casula *et al.*, 2024; Cuccuru, Fais, and Ligas, 2014). V_{pf} represents the average ultrasonic pulse velocity measured in every ashlar, and V_{pi} is the value of speed of the quarry fresh specimens namely 3700 m/s for the coarse-grained granitoid and 2800 m/s for fine-grained granitoid.

This index provides a quantitative means to evaluate material degradation and, consequently, to classify the quality of building materials (QBM). According to this scale, Velocity Ratio Index values below 0.25 indicate very poor material condition, typically associated with severe internal damage or loss of cohesion. Values between 0.25 and 0.50 correspond to poor quality, reflecting moderate to significant deterioration. The range of 0.50 to 0.75 is considered fair, indicating materials that are partially degraded but still structurally serviceable. Velocity Ratio Index values between 0.75 and 0.90 classify materials as good, while values above 0.90 represent very good condition, suggesting minimal to no alteration when compared to the reference intact stone.

4.3. Digitalisation

The surveying phase involved the comprehensive collection of data using both terrestrial and aerial methods. In this study, terrestrial images were captured using a Nikon Z6 II camera equipped with a 24-70 mm f/2.8 lens. Despite the lens's zoom capability, the focal length was kept constant at 24 mm with a fixed aperture. A total of 1382 images were acquired, 1192 of which were selected for alignment after quality filtering. Aerial data for both interiors and exteriors were collected using a DJI Mavic 2 Pro UAV, equipped with a Hasselblad L1D-20c camera featuring a 1" CMOS sensor (20 MP). This camera provides a field of view of approximately 77° (28 mm equivalent focal length) and an adjustable aperture range from f/2.8 to f/11. In total, 2,043 aerial images were collected, with 1525 successfully aligned.

This stage ensures the geometric and semantic accuracy of the resulting Heritage Building Information Model. The integration of multi-scale, multi-source surveys was facilitated through precise preliminary geo-referencing and the placement of Ground Control Points (GCPs). To ensure the seamless alignment of datasets from different cameras and to support the transition from exterior to interior environments, seven GCPs were strategically placed both around and inside the building. All photosets were oriented using Agisoft Metashape Pro (v. 2.2). To optimize the quality of the point cloud, the sparse point cloud was refined following the methodology proposed by Over *et al.* (2021). The following metrics were achieved:

- RMS reprojection error: 0.318 (0.779 pix)
- Max reprojection error: 2.2689 (7.94885 pix)
- Mean key point size: 2.40364 pix
- Average tie point multiplicity: 7.45847

A dense point cloud consisting of 241864735 points, with a camera visibility range of 3 to 132 after confidence filtering, was generated from depth maps. The point clouds were scaled using site-measured distances between GCPs. A pre-processing stage followed, including clipping, decimation, and segmentation of the point set.

Micro-photogrammetry was performed on specific elements of the monument, including a lesion on the entrance lintel and three wall sections (100 cm² each) affected by stone decay. These surveys were conducted using a Nikon D3300 camera with an 18-55 mm lens and 24 MP resolution. Each reconstruction involved 60 to 80 photos, depending on the spatial complexity of the sample. A digital caliper (0.1 mm tolerance) was used to obtain measurements for scaling the Digital Elevation Model (DEM). Each area was marked with a physical mask to ensure the exact repositioning of the scanned surface in subsequent surveys. This step is critical for replicating the photogrammetric survey for ongoing monitoring and diagnostic analysis. All processing was carried out using Agisoft Metashape Pro (v. 2.2).

4.4. Heritage-Building Information Modelling methodologies

As a preliminary approach to the study of the chapel, a low Level of Detail HBIM model was developed to support the integration and visualization of semantic information related to stratigraphic research and building material analysis thematic maps. The choice of using low Level of Detail is related to the flexibility and lightness, allowing an interdisciplinary group of stakeholders to easily interact with the model. The focus of this study is on the stone elements which compose the walls and floor of the chapel. Therefore, the approach described herein can be seen as a step in a documentation process that leads to a higher Level of Detail model.

VisualARQ and Rhino were used as Building Information Modelling authoring platforms for importing the point clouds, creating parametric object, and interactive modelling of building elements. Although this platform supports UV coordinate generation for texture mapping it currently does not export UV Maps to Industry Foundation Classes (IFC) format. Hence, semantic classification and UV Mapping were conducted in Blender, using BonsaiBIM 0.8.3 (formerly BlenderBIM), which allows native authoring of IFC, as well as scripting with the ifcopenshell library.

The proposed approach involves using geometrical proxies aligned with the parametric object representation, as proposed by Solla *et al.* (2020). These duplicated geometries were exported as independent IfcBuildingElementProxy entities geometrically coincident with the original BIM elements. The original architectural objects (e.g., IfcWall) were preserved as the primary semantic architectural representation, while the proxy objects acted as carriers for thematic information such as stratigraphic interpretation, building material quality mapping, ultrasonic testing, or architectural phasing (ARQ). This strategy avoids the need for permanent geometric subdivision of the architectural model when multiple non-coincident analytical interpretations coexist.

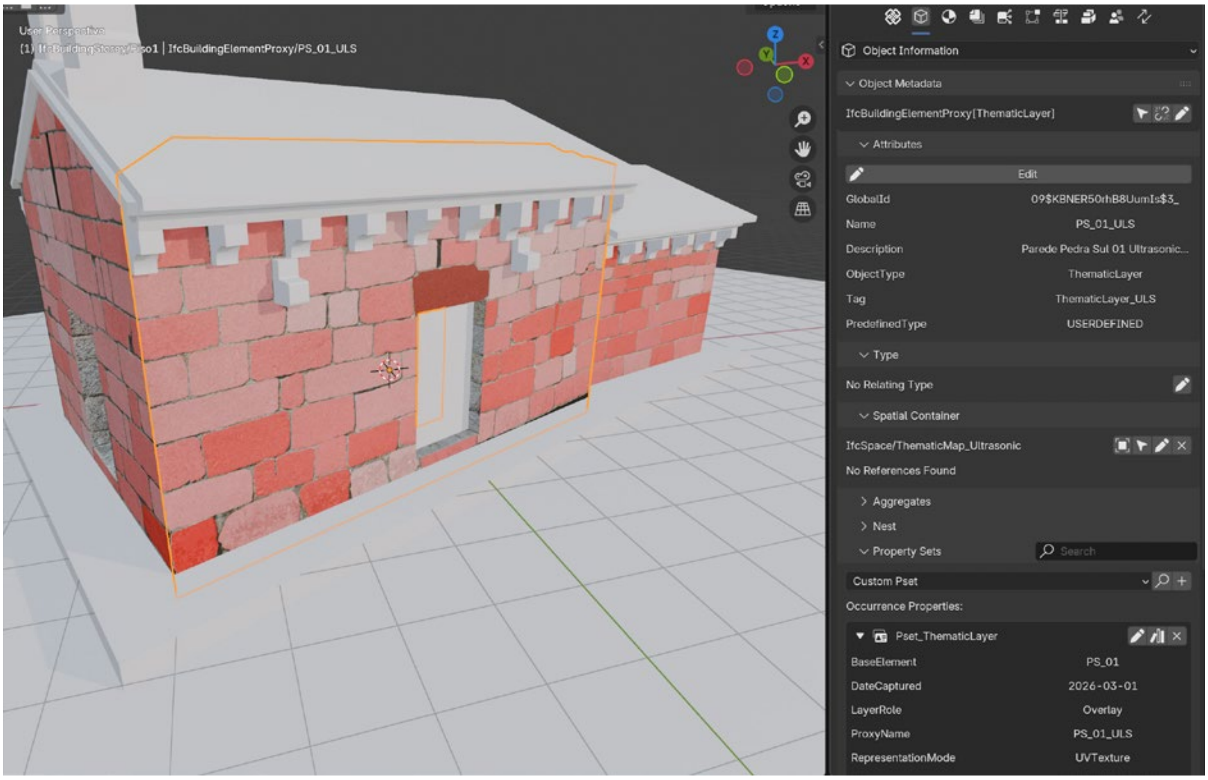

Figure 2. Building model showing a proxy object metadata classified as ifcBuildingElementProxy, and the respective custom Property Set. Digital processing by authors.

The classification of these thematic layers as IfcBuildingElementProxy provides the flexibility to encode non-standard information without compromising IFC model validity. Each proxy was assigned a USERDEFINED predefined type and accompanied by a custom property set and external references linking to the original images (Fig. 2).

The thematic mapping workflow relied on tessellated mesh representations and UV texture mapping. Proxy geometries were triangulated prior to export and represented in IFC using IfcTriangulatedFaceSet. UV coordinates were associated with the tessellated geometry through IfcIndexedTriangleTextureMap and IfcTextureVertexList. The thematic maps themselves were stored as external PNG image files referenced through IfcImageTexture. Texture definitions were associated with the proxy geometry through IfcSurfaceStyleWithTextures, linked to the corresponding IfcSurfaceStyle and assigned to the proxy representation through IfcStyledItem relationships, allowing each thematic layer to be independently represented while preserving the original architectural geometry.

The texturing workflow involved the following steps outlined by SirreJ in 2022:[3]

1. Create an ifcMaterial for each combination of thematic map and wall and assign it to the corresponding IfcBuildingElementProxy
2. An IfcSurfaceStyle was created for each thematic layer and associated with the corresponding IfcMaterial and proxy representation
3. Triangulation of proxy geometries using the *Geometry and Materials > Force Triangulation option*
4. UV unwrapping of proxy meshes using *Smart UV Project* tool to generate UV coordinates for texture projection
5. Creation of materials definition and assignment of textures to corresponding UV maps
6. Export of UV coordinates and texture references to IFC using BonsaiBIM and ifcopenshell scripting workflows

Semantic classification is enriched by using two strategies:

1. Custom property sets (*IfcPropertySet*) were created to encode structured metadata including theme type, data collection date, data collector, and associated wall ID
2. External References (*IfcDocumentReference*) were created to link original image files to the relevant *IfcBuildingElementProxy* instances via *IfcRelAssociatesDocument* but can also be used for diagnostic reports or other relevant data

5. RESULTS AND DISCUSSIONS

5.1. The construction sequence of S. João de Calvos

The working method was based on the *in situ* differentiation of stratigraphic units (SU, Annex SF1), documented on both the exterior and interior of the church. The tasks of correlation, synthesis, and dating made it possible to group the SU into Activities (A) and Phases (Annex SF1), and to construct the stratigraphic sequence (Annex SF2). The SU (Figs. 3, 4, 5) and the Phases (Figs. 6, 7, 8) were represented on a graphical documentation, produced from the photogrammetric model. This analysis enabled the identification of three construction phases organized into several sub-phases, which are described below.

[3] https://github.com/SirreJ/UV-mapping-IFC-BlenderBIM/blob/main/Uv_mapping_IFC_step_by_step.pdf

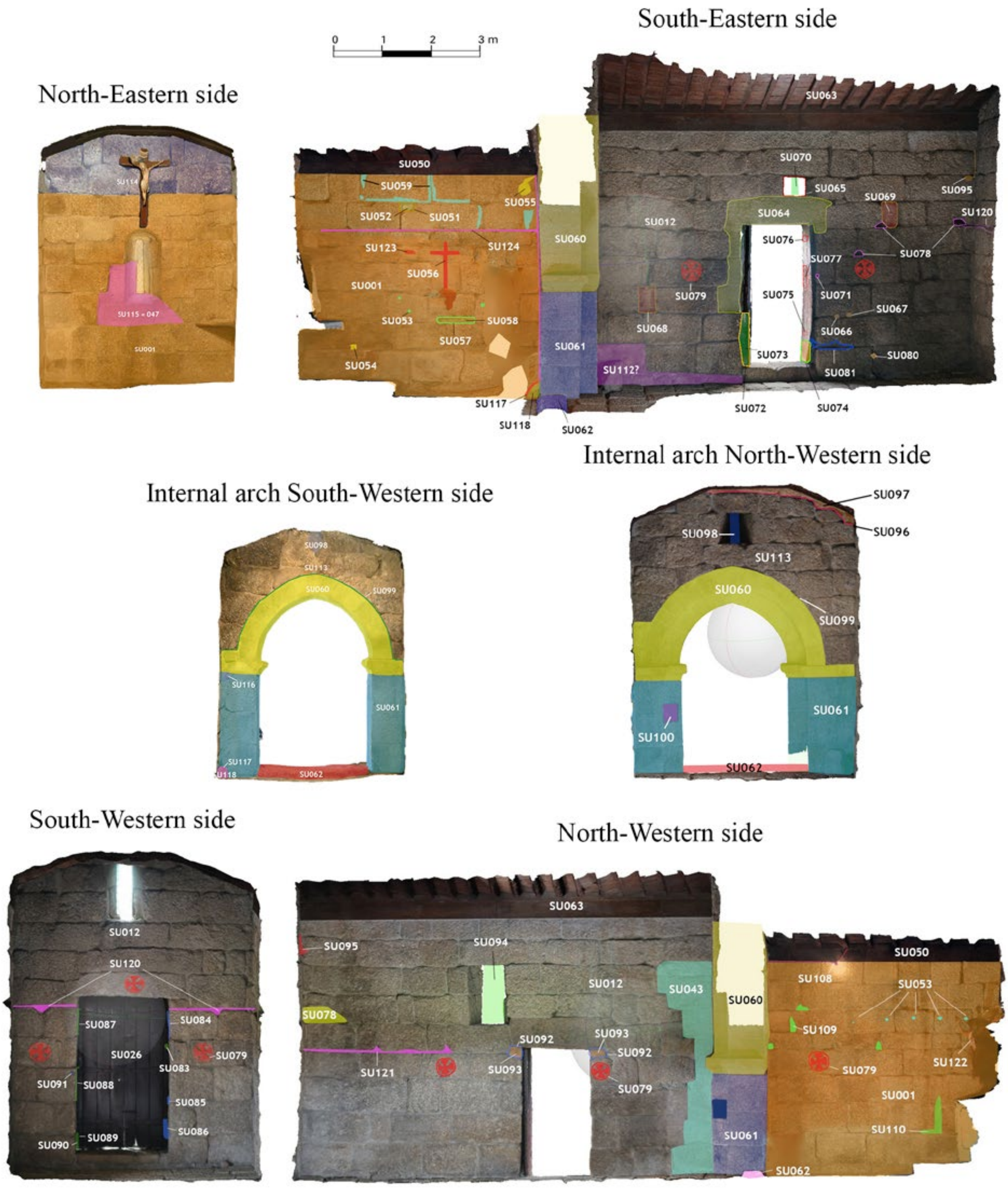

Figure 3. View from inside the church of the various walls with relative indications of the SU.
Digital processing by authors.

5.1.1. Phase I: Middle Ages, 12th–14th centuries

This phase corresponds to the initial construction period, although the analysis reveals two distinct moments: the apse, locally known as the *capela-mor*, as well as the remains of an earlier nave, of which only some foundation vestiges are preserved (Phase Ia). A subsequent remodelling of the nave led to the enlargement of the original church (Phase Ib). It is unclear whether this was due to the collapse of the first nave or to the need to increase its size. The nave’s orientation differs from that of the apse, and possibly, from the original nave, as can be seen in Fig. 4. The distinctions between these two phases are evident in three key aspects: their orientation, the distinct construction techniques employed, and the typology of the corbels.

5.1.1.1. Phase Ia: Apse and remains of an earlier nave. Pre-1220, possibly late 12th to early 13th century

This sub-phase includes three Activities.

A100 (SU001, 007, 043, and 113) corresponds to the construction of the main chapel and the beginning of the original nave. The main chapel (SU001) has a rectangular floor plan, oriented approximately E–W, and is built in regular granitoid ashlar laid in horizontal courses; however, the two uppermost courses are narrower than the rest. It includes a row of cavetto-type corbels, some decorated with geometric motifs, and a cornice with a double moulding. A narrow-slit window on the north-eastern elevation, which was partially blocked (SU047–SU115), is also included. The remains of the earlier nave (SU043) display the same construction technique as the apse (SU001); they are only visible on the interior and exterior north-western elevation and are separated from the wall of Phase Ib (SU012) by a stepped cut (SU042). Also belonging to this phase are the remains of the presbytery wall (SU113), preserved above the chancel arch built in Phase Ib, and constructed using the same technique as walls SU001 and SU043. This activity also includes the antefix cross (SU007), a simple cross inscribed within a circle crowning the roof.

A101 (SU104 and SU105) corresponds to the apse floor, composed of granitoid slabs (SU104) of varying size and shape, with a raised north-eastern section (SU105), sharing the characteristics of SU104.

Finally, **A102** (SU107) corresponds to the base of the original altar, consisting of a reused *ara* with a space for a lipsanoteca (reliquary), SU107), an element commonly found in medieval altars where materials from earlier periods were reused.

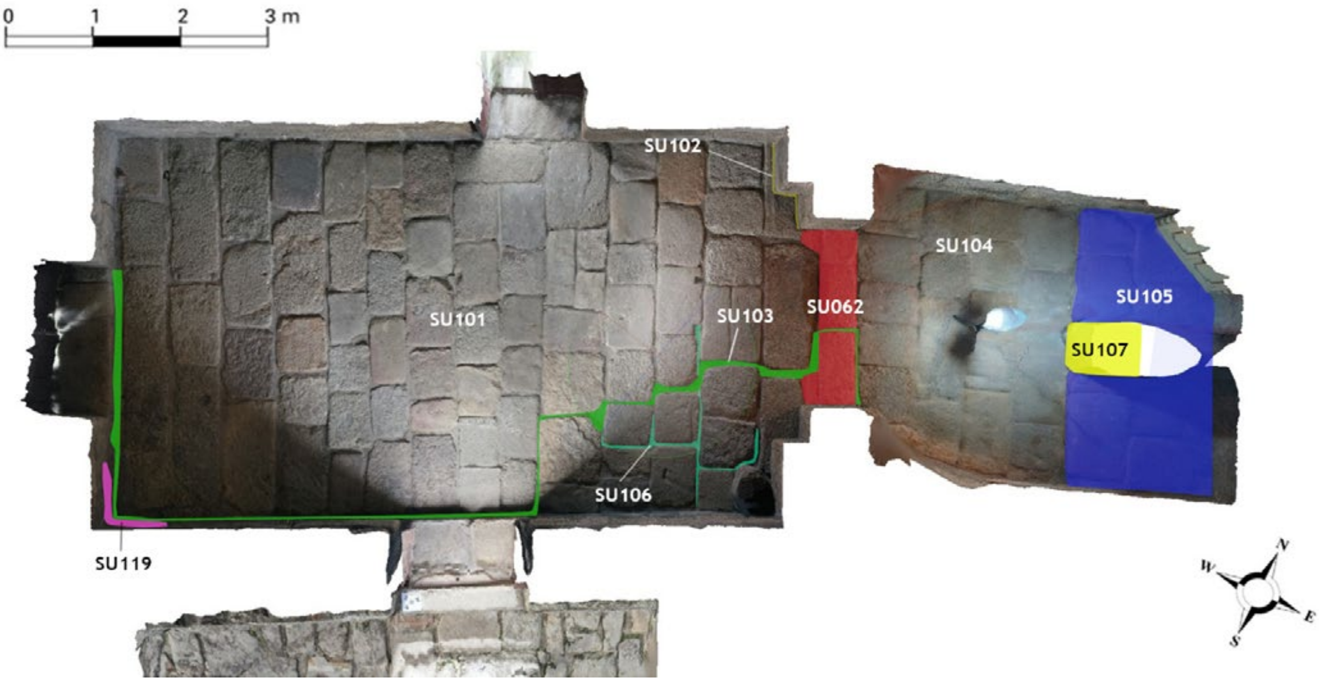

Figure 4. View from above of the church floor with relative indications of the SU.
Digital processing by authors.

5.1.1.2. Phase Ib: Remodelling/enlargement of the nave and south-side portico. 13th–14th centuries

Figure 5. View from outside the church of the various walls with relative indications of the SU.
Digital processing by authors.

In this sub-phase, seven Activities have been identified.

A103 (SU012, 013, 042, and 112) corresponds to the construction of the nave. Among the identified elements is a base course (SU013 and 112) supporting the nave wall (SU012), visible on the exterior south-eastern elevation and, in the case of SU112, also on the interior. It is composed of granitoid ashlars of greater height than those of wall SU012, projecting from the wall and only roughly dressed, thus resembling a plinth. On the exterior, it can be observed that there may have been another course below this one. The nave also has a rectangular plan and is built in granitoid ashlar masonry; however, it features courses of irregular height, many of them slightly sinuous rather than fully horizontal, and includes some headers and wedges. The ashlars are not regular, and some appear to have been reused. The cavetto-type corbels in this phase are wider and rougher than those of the apse, and the cornice has a simple square-section moulding. The cut of the original nave (SU042) on the north-western elevation has also been included in this activity, where the courses differ in height from those of Phase Ia, indicating they belong to different phases.

A104 (SU060, 061, 098, 099, and 102) corresponds to the renovation of the entrance arch to the main chapel. During this sub-phase, the chancel arch was also remodeled by cutting into the previous wall (SU099) and the floor (SU102) in order to construct a pointed arch (SU060) with a central keystone, supported on cavetto-type imposts (a feature characteristic of the early Gothic) resting on piers (SU061).

A105 (SU101) corresponds to the construction of the nave floor, composed of irregular granitoid slabs which are, in general, roughly quadrangular in shape and arranged in courses running north–south. In some cases, the courses narrow and consist of two granitoid pieces instead of one. Some slabs are reused elements bearing different types of marks. As in the case of the apse, this would correspond to the original floor. The blocking of the lower part of the slit window located above the original chancel arch (SU098) has also been included in this activity.

A106 (SU015, 016, 017, 018, and 019) corresponds to the construction of a portico attached to the south-eastern façade of the nave. Of this structure, two granitoid corbels used to support a beam running parallel to the wall are preserved, along with two cuts above the corbels for the supporting beams of the roof inserted into the wall. In addition, four beam holes beneath the eaves of the cornice were identified for the placement of the sloping roof beams, which are of smaller section than the former. All beam holes are quadrangular.

A107 (SU079) corresponds to the execution of a *Via Crucis* on the interior walls of the church, of which nine Maltese crosses engraved in the ashlar masonry are preserved, inscribed within circles and showing traces of red pigment. These are found on both the nave and apse walls.

A108 (SU021) corresponds to a cut documented in the nave, whose function remains unknown.

Finally, **A109** (SU 075, 076, 083, 091) corresponds to the earliest wooden doors fitted into the north-western and south-western openings, consisting of various cuts in the jambs (SU075, 083, and 091), as well as the hinges of a former door in the south-eastern opening of the nave.

5.1.2. Phase II: Early Modern Period, 15th–16th centuries

This phase corresponds to a series of transformations carried out at the beginning of the Early Modern period, among which the construction of the bell gable and the south-west facing portico stand out. It has no sub-phases, and nine Activities have been identified.

A200 (SU030, 031, 032, 033) corresponds to the construction of the bell gable on the south-western façade. For this purpose, cuts were made into the cornice of the façade (SU030), upon which two granitoid bases (SU031) were placed, and the bell gable (SU032) was erected. It is built with granitoid ashlar piers of square section, topped by an impost supporting a pointed arch with a central keystone. Within this, a cast-iron bell (SU033) is located beneath a wooden support.

A201 (SU029) is interpreted as the construction of a portico on the south-western façade. It consists of six beam holes, three of square section and the other three irregular, distributed across the entire width of the façade at three different heights: three aligned above the doorway, two aligned at the sides of the lintel, and one in the same vertical line as the beam hole located to the left of the lintel. Based on both their configuration and location, they may have had a dual function: supporting a porticoed structure in front of the façade and providing access to the bell gable for maintenance purposes.

A202 (SU027) corresponds to the abrasion tracks left by the friction of the rope used to ring the bell, between the cornice and the door lintel. This action caused alterations to the slit window located above the door, as well as a crack in the lintel.

A203 (SU071, 072, 073, 074, 077, and 081) corresponds to the remodelling of the south-east door of the nave, evidenced by a series of cuts documented in its jambs (SU071, 072, 074, 077) and on the right side of the doorway (SU081), as well as the filling of some of these cuts (SU073).

A204 (SU084, 085, 086, 087, 088, and 089) corresponds to the remodelling of the south-west door of the nave, indicated by a series of cuts documented in its jambs.

A205 (SU092) corresponds to the remodelling of the north-west door of the nave, represented by a cut interpreted as the possible removal of a previous lintel.

A206 (SU078, 120, and 121) corresponds to the construction of a high choir at the western end of the nave, above the main entrance to the church. The surviving evidence consists of a series of beam holes located on the north-western and south-eastern elevations for the placement of beams supporting the floor and access and fastening elements, as well as two chases cut into the north-western, south-western, and south-eastern walls (SU120, 121), corresponding to the insertion of the floor into the walls.

A207 (SU114) corresponds to the repair of the north-eastern wall of the main chapel, possibly related to a modification of the roof. It is composed of two courses of granitoid ashlar masonry laid in stretcher and header, with perfectly regular courses.

Finally, **A208** (SU100) corresponds to the installation of a wooden donation box on the wall of the chancel arch.

5.1.3. Phase III: Contemporary Period, 20th–21st centuries

Following an extended period of neglect, a series of interventions aimed at improving the facilities and rehabilitation of the church began in the 20th century and continued into the early 21st century. Four construction sub-phases have been identified.

5.1.3.1. Phase IIIa: Interior renovations and limewash, pre-1952

In sub-phase IIIa, four Activities have been identified.

A300 (SU049, 053, 054, 055, 066, 067, 108, 116, 117, and 118) corresponds to the installation of a lighting system in the main chapel, evidenced by a series of perforations and chases made to accommodate electrical wiring, light switches, and lamps.

A301 (SU080, 095, and 119) corresponds to the installation of a lighting system in the nave, also reflected in a series of perforations and chases made to accommodate electrical wiring in the walls and floor, as well as switches and lamps.

A302 (SU009 and 059) corresponds to the limewashing of the church, with traces of lime preserved both in the interior (SU059) and the exterior (SU009).

Finally, **A303** (SU056) corresponds to the installation of wooden liturgical elements in the main chapel, of which a pedestal and a cross on the south-eastern elevation (SU056) have been preserved.

5.1.3.2. Phase IIIb: Cracks and structural damage due to abandonment (1950–1970)

Sub-phase IIIb has been associated with **A304** (SU004, 005, 028, 044, 046, and 111), which corresponds to a series of cracks and breaks resulting from the abandonment and lack of maintenance of the building. Cracks typically occur in elements that have been affected over time by different actions, such as the friction of the bell rope, which causes damage to the door lintel (SU028), or in vulnerable and exposed areas such as eaves (SU005), corbels (SU004), and lintels (SU044), as well as in deteriorated ashlars (SU046, 111). It is noteworthy that all these features have been documented on the exterior of the building, indicating the greater exposure of the outer façades to various forms of decay.

5.1.3.3. Phase IIIc: Direcção Geral dos Edifícios e Monumentos Nacionais's restoration, post-1970

In this sub-phase, a series of interventions were carried out by the *Direcção Geral dos Edifícios e Monumentos Nacionais* (Portugal), which define the building's current state, although the roof has also been modified at a later stage. Seven Activities have been identified.

A305 (SU022, 034, 038, 039, 040, 041, 051, 052, 057, 058, 090, and 098) includes a series of unspecified recesses (SU038, 040, 041, 051, 057) and their corresponding repairs and fillings of interfaces opened in earlier phases (SU022, 034, 039, 052, 058, 090), typically carried out using small stone blocks and Portland cement. This activity also includes the blocking of the window opened above the chancel arch (SU098).

A306 (SU047, 048, 065, 070, 082, 094, and 115) corresponds to the opening or modification of a series of windows in the nave and their closure with glass. The slit window in the apse was partially blocked with a stone (SU047–SU115) and fitted with glass (SU048). A small window was opened above the south-east door (SU065) and closed with glass (SU070), as were the remaining windows (SU082, 094).

A307 (SU024, 026, 036, 064, and 093) corresponds to the renovation of the wooden doors. It includes a series of cuts made to install these new doors on the north-western elevation (SU064, 093), as well as the placement of three rectangular wooden doors on the north-western, south-western, and south-eastern façades (SU024, 026, 036).

A308 (SU002, 003, 014, 025, 035, and 106) corresponds to a series of interventions on the interior and exterior pavements of the church. On the exterior, a pavement or walkway (SU003) was laid around the church, which in some areas is bonded with cement to the façades (SU002). Raised thresholds were also installed at the three doorways (SU014, 025, 035), possibly to prevent water ingress, as the interior floor level is lower than the exterior. This activity also includes the repointing of the nave floor joints with cement (SU106). The threshold beneath the entrance to the chancel arch was also repaired.

A309 (SU103) corresponds to the installation of new electrical wiring in the floor of the church, using the joints of the paving. It runs from the main chapel to the south-west door.

A310 (SU010, 050, 063, 096, 097, and 098) corresponds to the repair of the church roof. This includes part of the nave's gabled roof covered with arabic tiles (SU010), as well as the wooden coffered ceilings of both the nave (SU063) and the main chapel (SU050). In both cases, the central section is flat while the sides are sloping; they rest on a main beam supported by the north and south-eastern elevations and include rafters upon which the boards supporting the roof covering are laid. To install this roof, the presbytery wall was raised using masonry bonded with cement (SU096, 097), which also entailed the blocking of the window in that same wall (SU098).

Finally, **A311** (SU020) involves the repointing of the joints of the church's exterior façades with cement, which is preserved only intermittently.

5.1.3.4. Phase IIId: Roof renovations, late 20th–early 21st century

The most recent sub-phase corresponds to a single activity, A312 (SU006, 008, 011, and 045), which involved the partial repair of the nave's tiled roof (SU011) and the complete repair of the apse roof (SU006), using the same type of tiles as those employed in sub-phase IIIc. In addition, the junction between the apse roof and the exterior wall of the presbytery was sealed with cement and a metal plate (SU008, 045) for preventing water infiltration into the church.

5.1.4. Undetermined

Finally, several stratigraphic units were recorded but remain undated or with unclear functions. These are SU021, 023, 037, 038, 040, 051, 068, 069, 109, and 110, all of which are cuts or interfaces.

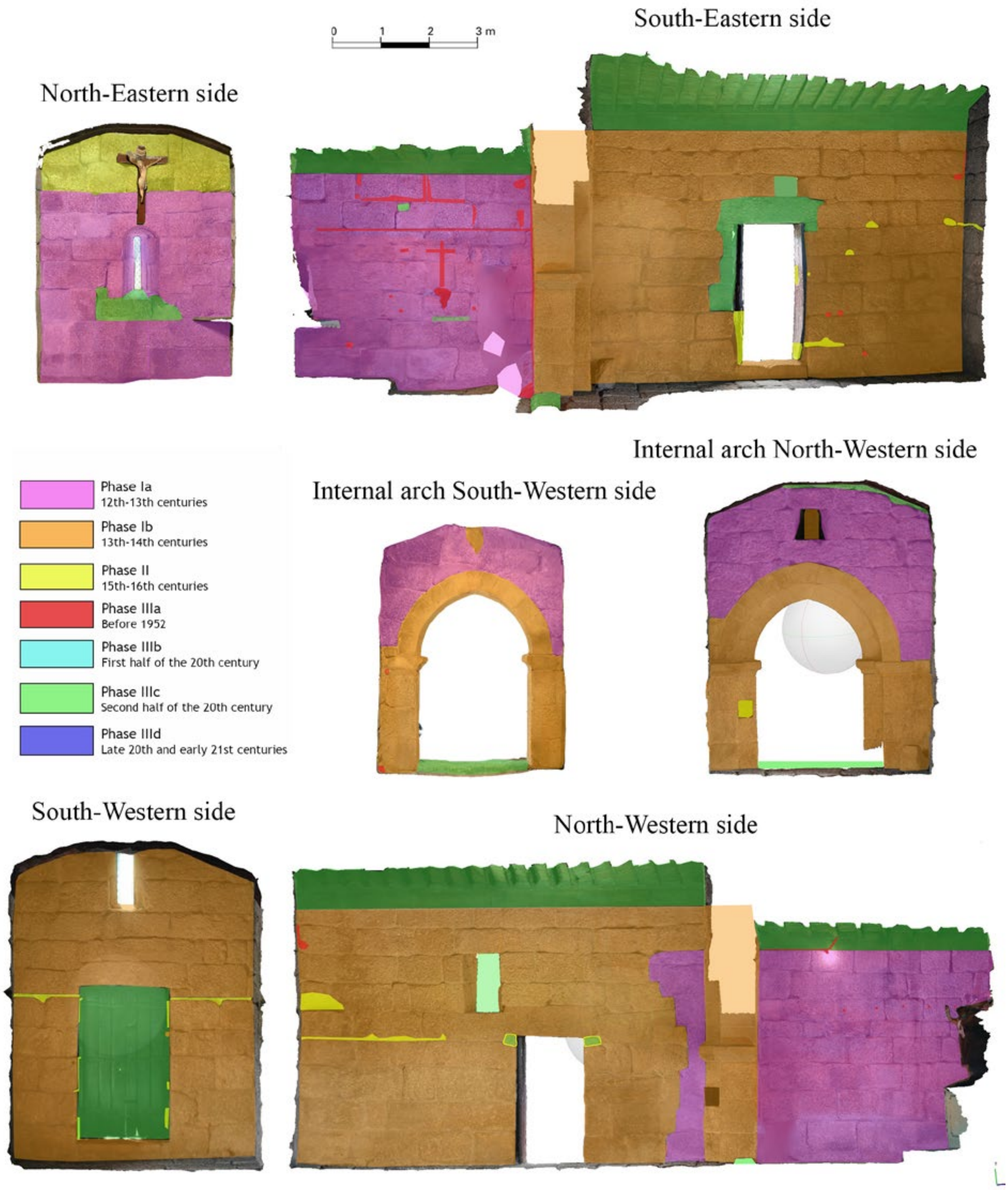

Figure 6. View from inside the church of the various walls with relative indications of the construction phases. Digital processing by authors.

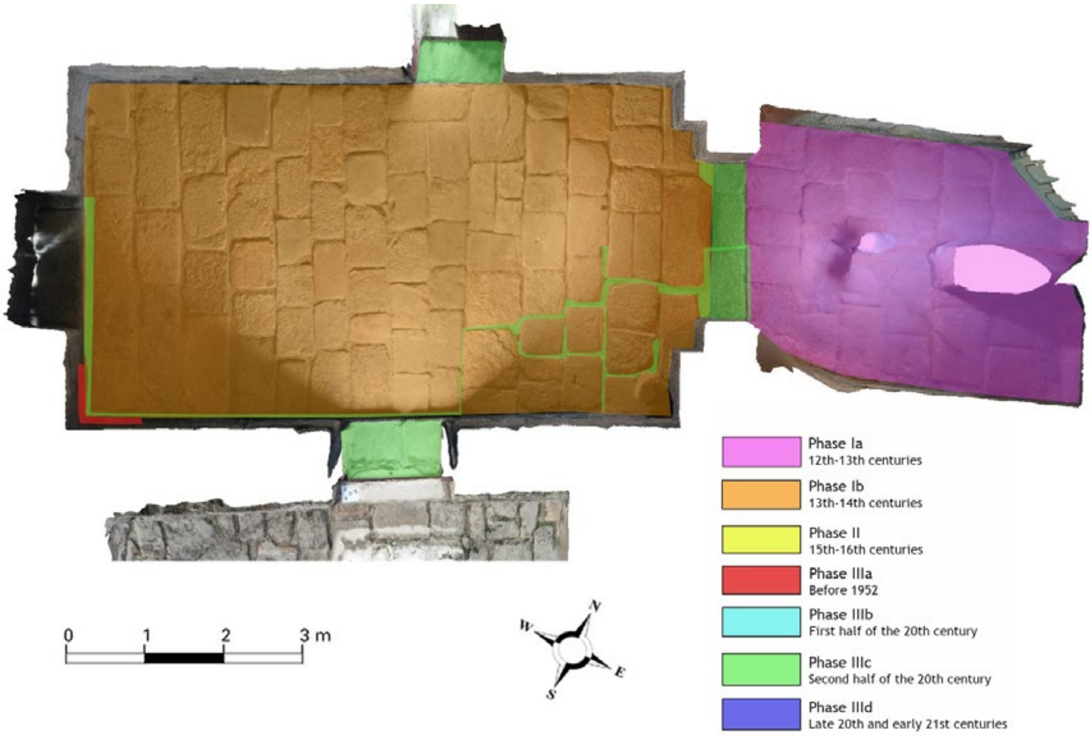

Figure 7. View from above of the church floor with relative indications of the construction phases. Digital processing by authors.

Figure 8. View from outside the church of the various walls with relative indications of the construction phases. Digital processing by authors.

5.2. Building materials analysis

A detailed analysis of the building materials was undertaken to characterise the current weathering phenomena, to understand the performance and compatibility of past repair interventions, and to establish a scientifically grounded baseline that can support future conservation and maintenance strategies, even though the monument does not presently exhibit a critical level of deterioration.

As shown in Fig. 9, the church, in its current state, is characterised by three main construction materials: blocks of two different types of granitoid, which will be discussed later, bonded together with Portland cement. The latter was poured and spread during the restoration work carried out by the local *Direcção-Geral dos Edifícios e Monumentos Nacionais* after 1970 (Phase IIIc). The cement fillings were most likely applied due to the deterioration of the original bedding mortar, which in monuments from that period was often air-lime type and poorly resistant to weathering processes. It is believed that the mortar experienced significant washout and disaggregation, which exposed the edges of the ashlars. This issue is quite common and has also been observed in other buildings of the same age (Sitzia, 2024).

Additionally, the church was constructed using two different types of granitoid. About 10% of the structural elements, such as ashlars and corbels, particularly those with decorative or artistic features, are made of fine-grained granitoid. The remaining approximately 90% consists of coarse-grained granitoid, mainly used for larger blocks. Some corbels on the north-western side are also crafted from this stone.

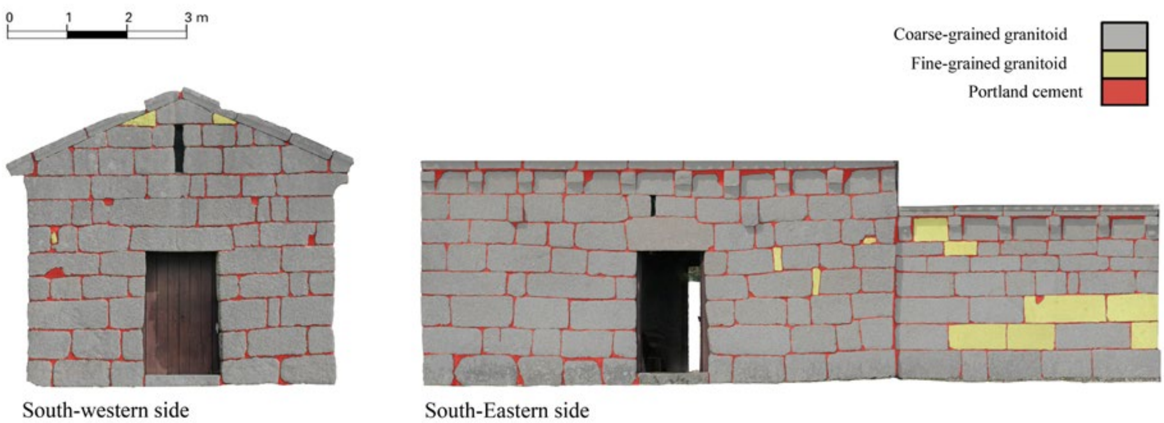

Figure 9. Results of the ashlar's geological mapping across the south-western and south-eastern side of the church. Digital processing by authors.

The analysis of the two granitoids in thin section is shown in Fig. 10a and 10b, while Table 1 presents some basic physical properties of the fresh stone. According to the geological map provided by the *Laboratório Nacional de Energia e Geologia*, the coarse-grained granitoid used in the church is described as *Guimarães-Santo Tirso* biotitic granitoid and coarse-grained porphyritic monzogranites, belonging to the late-tectonic Hercynian lithologies.

The provenance of the fine granitoid could be attributed to the fine-grained monzogranite of *Fafe-Sendim* or the *Santo Antão* granite. Determining the exact origin of this stone is still underway. In any case, all the lithotypes are local and outcrop near the church.

Within the building, sparse ashlars of both coarse and fine-grained granitoids are characterised by "golden *facies*," displaying a warm, golden hue caused by the alteration of ferro-magnesian minerals. These originally dark minerals undergo chemical weathering and alteration processes, which produce the distinctive golden or yellowish tones. These granites, in outcrop, are frequently associated with hydrothermal activity and fault zones with circulating fluids that accelerate mineral alteration.

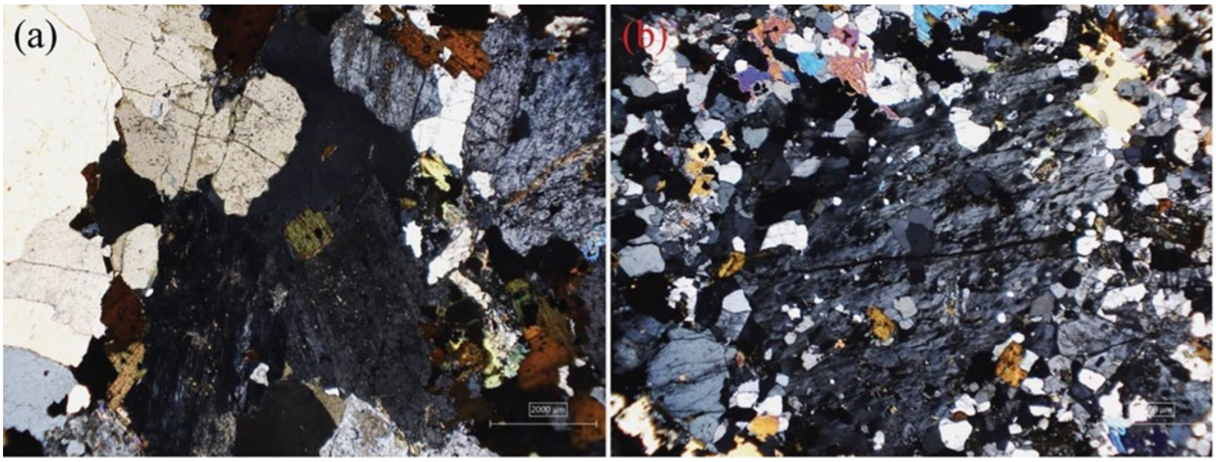

Figure 10. Thin section of coarse-grained granitoid (a) and fine-grained granitoid (b).
Both photographs were taken by crossed nicols. Photos from authors.

In any case, it is not possible to identify the precise location of the ancient quarry, nor to hypothesize two different supply quarries. In fact, these lithologies can outcrop within short distances while being in contact with each other. Moreover, as often happens in medieval constructions, the use of erratic boulders was frequently employed (Czubla *et al.*, 2024; Górska-Zabielska, 2024).

The two stones certainly present similar properties in terms of workability, hardness, and cleavability, differing instead in durability and carvability. This difference is much more pronounced in the fine-grained facies, allowing for the easier production of artistic elements such as corbels. However, these elements are also made using the coarse-grained facies which, despite its lower carvability, is still well suited for this type of architectural element. In the past, the use of coarse-grained stones to produce artistic elements did not seem to pose a problem. In Portugal, an example is the *Trigaches* marble, used in various historical periods and comparable in grain size to the coarse-grained granite present in the church (Rosa *et al.*, 2023).

In the building there is no clear evidence that allows the use of one stone or the other to be attributed to a specific construction phase. The fine-grained granite appears to have been used more frequently in Phase Ia; however, some scattered ashlars are also present in areas of the building associated with Phase Ib. It should be emphasized that the use of different lithologies does not reflect aesthetic requirements, since the building was originally rendered with multiple mortar layers, with a probable thickness on the order of 5 cm.

Both granitoids appear to be affected by various weathering processes, both meteoric and biological. In some cases, granular disintegration of the coarse-grained granitoid is very advanced. Additionally, rare but observable exfoliation phenomena also affect this lithology. In contrast, the fine-grained granitoid does not appear to be subject to this type of weathering.

The more advanced weathering of the coarse-grained granitoid is primarily controlled by its textural features, and only secondarily by the physical properties reported in Table 1. Although helium open porosity (one of the parameters influencing decay, Lisci *et al.*, 2023) is lower than in the fine-grained granitoid (3.36 ± 0.49 % *vs* 10.72 ± 1.79 %), and water retention properties (0.99 ± 0.10 % *vs* 3.20 ± 0.45 %) are more favourable, the large crystal size and lower intergranular cohesion promote grain detachment and sanding, leading to greater susceptibility to alteration. To assess the current decay state of both stones, a comprehensive ultrasonic pulse velocity survey was conducted across the four main elevations. An example of the survey conducted on the elevations south-western and south-eastern is illustrated in Fig. 11.

According to the survey, the coarse-grained granitoid ashlars show average ultrasonic velocities of 1060 m/s on the south-western façade, 1267 m/s on the north-eastern façade, 1140 m/s on the north-western façade, and 1170 m/s on the south-eastern side. These values should be compared with the ultrasonic velocity of the same lithology measured on fresh quarry samples (~ 3700 m/s).

In contrast, the fine-grained granitoid ashlars show average values of 1830 m/s on the south-western façade, 1570 m/s on the north-eastern façade, 1580 m/s on the north-western façade, and 1467 m/s on the south-eastern façade. Again, these values should be compared with the ultrasonic velocity measured on fresh quarry samples of the same stone (~ 2800 m/s).

Table 1. Physical features of coarse-grained granitoid and fine-grained granitoid. Data from authors.

Lithology	Real density (g/cm^3)	Imbibition coefficient (%)	Bulk density (g/cm^3)	Helium open porosity (%)	Water open porosity (%)	Saturation index (%)
Coarse-grained granitoid	2.65	0.88	2.57	3.05	2.26	73.96
	2.64	0.91	2.57	2.91	2.33	80.14
	2.65	1.13	2.55	4.10	2.89	70.44
	2.65	1.05	2.56	3.12	2.69	85.96
	2.72	0.96	2.62	3.61	2.52	69.91
Average	*2.66*	*0.99*	*2.57*	*3.36*	*2.54*	*76.08*
S.D.	*0.03*	*0.10*	*0.03*	*0.49*	*0.26*	*6.86*
Fine-grained granitoid	2.71	3.69	2.40	11.50	8.84	76.88
	2.75	2.73	2.47	10.36	6.75	65.12
	2.71	2.96	2.34	13.42	6.92	51.61
	2.73	2.94	2.48	9.17	7.29	79.51
	2.70	3.69	2.45	9.17	9.03	98.43
Average	*2.72*	*3.20*	*2.43*	*10.72*	*7.77*	*74.31*
S.D.	*0.02*	*0.45*	*0.06*	*1.79*	*1.08*	*17.43*

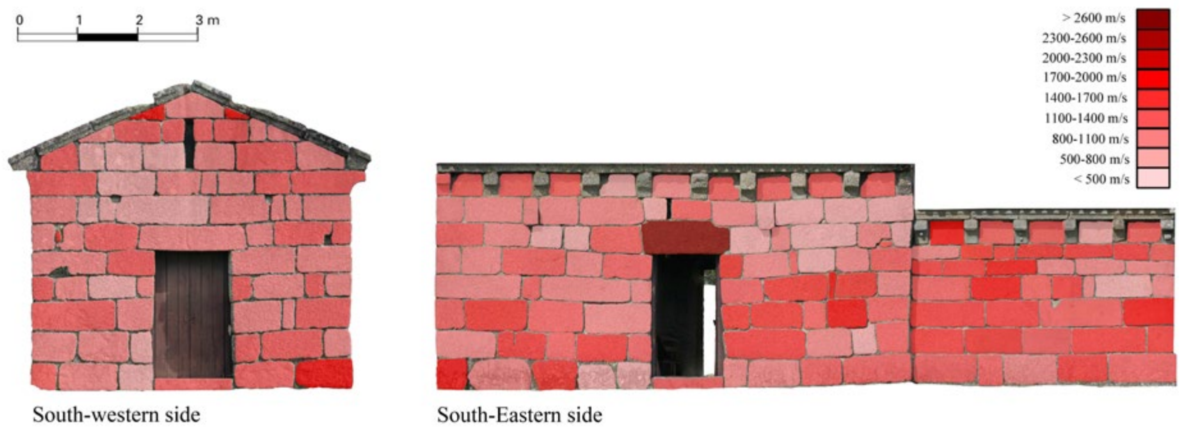

Figure 11. Results of the ultrasonic survey across the south-western and south-eastern side of the church. Digital processing by authors.

As explained in the methods section, Kahraman, Ulker, and Delibalta (2007) provide a practical and quantitative basis for interpreting ultrasonic test results, enabling the identification of priority zones for conservation interventions, and supporting a systematic approach to heritage material assessment. For each ashlar, a Velocity Ratio Index was calculated using reference values measured from fresh quarry specimens. The Velocity Ratio Index provides a normalized module of material integrity and allows classification into categories. The results were grouped by elevation to allow comparative assessment across different sections of the structure (Table 2, Fig. 12).

5.2.1. South-western elevation — *Most Degraded*

This façade presents the lowest average Velocity Ratio Index (0.54), with only 2.9% of ashlars classified as “Good or very good” and a notable 20.6% rated as “Poor or very poor.” The remaining 76.5% fall within the “Fair” category, indicating generalized but not critical degradation. These results are consistent with visual assessments that revealed surface scaling, advanced granular disintegration and biological crusts.

This orientation is particularly vulnerable due to a combination of factors: prevailing westerly winds, higher exposure to driving rain, and limited morning sunlight which delays drying cycles (Lisci *et al.*, 2022). Moreover, the structural damage identified in the lintel beneath the bell gable, previously documented via micro-photogrammetry, reinforces the need for immediate stabilization and continuous monitoring. The material in this zone is not only physically stressed by structural loading but also suffers from thermal gradients and water ingress.

5.2.2. North-western elevation — *Critical Zones Emerging*

With a mean Velocity Ratio Index of 0.57, the north-western elevation shows the highest proportion of “Poor or very poor” quality stones (24.4%) among all façades. Only 6% were classified as “Good or very good”, while the majority (69.6%) fall within the “Fair” category.

This degradation pattern reflects typical north-western exposure, characterised by limited solar radiation, persistent humidity, and extensive biocolonization. Additionally, evidence of historical interventions and repointing with Portland cement (identified in previous stratigraphic assessments) may have induced differential stress concentrations and microcracking, exacerbating decay in specific zones. Consequently, this façade should be considered a priority for non-invasive biocidal cleaning, water run-off improvement, and microstructural consolidation of the most degraded ashlars.

5.2.3. South-eastern elevation — *Intermediate Degradation*

Despite its southern orientation, this façade shows only a moderate state of conservation, with a mean Velocity Ratio Index of 0.57 and 16.8% of ashlars classified as “Poor or very poor.” The majority (79.4%) are in “Fair” condition, while only 3.7% fall into the “Good or very good” category.

Given its relatively favourable exposure, these results suggest the influence of localized pathologies rather than environmental factors alone. Potential contributors include thermal fatigue, particularly in stones with anisotropic thermal expansion, and architectural detailing that provides inadequate protection for joints or horizontal surfaces, thereby promoting water retention and salt crystallization. Although this façade does not exhibit severe generalized degradation, specific isolated zones would benefit from water-repellent treatments (or hydrophobic protection) and surface consolidation.

5.2.4. North-eastern elevation — *Best Preserved*

With a mean Velocity Ratio Index of 0.61, this façade shows the highest material integrity, with 6.9% of stones classified as “Good or very good” and only 12.1% falling into the “Poor or very poor” category.

These results confirm the preliminary visual inspection, which revealed limited biological colonization and minimal surface loss. The microclimatic conditions of this orientation, particularly balanced solar exposure and reduced wind-driven rain, appear to support the natural resilience of the materials. This façade may serve as a baseline for defining acceptable decay thresholds in future monitoring campaigns.

The distribution of ultrasonic velocities suggests a partial influence of façade orientation on the degree of weathering. In particular, the lower values recorded on the south-western façade, especially in the coarse-grained granitoid, likely reflect greater exposure to prevailing winds, driving rain, and solar radiation, all of which accelerate decay processes.

However, this pattern is not sufficiently consistent across all measurements to allow for a definitive interpretation. The observed variability is likely the result of multiple interacting factors, including local micro-exposure, differences in moisture retention, and the intrinsic textural properties of the stone. In particular, the higher susceptibility of the coarse-grained granitoid appears to remain the dominant control on degradation. No substantial differences between the two main construction phases (Ia and Ib) were identified based on the ultrasonic velocity analysis.

The combination of ultrasonic testing, Velocity Ratio Index classification, and façade-based spatial mapping provides a high-resolution understanding of decay processes in granitic heritage buildings. This diagnostic layer, integrated into the HBIM environment, enables targeted conservation planning and data-driven prioritization:

- The south-western and north-western elevations represent the zones of highest vulnerability and should be prioritized in early-stage conservation campaigns.
- The proposed differential photogrammetric survey technique, aimed at tracking material volume loss over time, should be focused on the most affected elevations, particularly around structural discontinuities such as lintels and joints.
- Integration of these results into the monument's HBIM model supports not only condition assessment but also long-term monitoring, simulation of deterioration scenarios, and optimization of resource allocation.

Overall, this façade-by-façade analysis demonstrates the critical importance of combining material science, non-destructive diagnostics, and digital workflows to support the sustainable management of historic stone buildings.

These results underscore the value of elevation-based analysis in diagnosing degradation trends in historic masonry. The Velocity Ratio Index and the quality of building materials, when integrated into Heritage Building Information Modelling of the church, supports a data-driven approach to preventive conservation. Risk-prone façades, such as the south-western and north-western elevations, should be prioritized in future interventions, which may include consolidation treatments, surface cleaning, and enhanced drainage. Moreover, the integration of ultrasonic pulse velocity and quality of building materials data into the HBIM model enhances spatial understanding of deterioration, enabling the development of customized conservation strategies for each elevation.

Table 2. Summary of ultrasonic survey results by elevation measured in every ashlar.

Elevation	Mean VRI	Poor or very poor (%)	Fair (%)	Good or very good (%)	Actual state
South-western	0.54	20.6	76.5	2.9	Most Degraded
North-western	0.57	24.4	69.6	6	Critical Zones Emerging
South-eastern	0.57	16.8	79.4	3.7	Intermediate Degradation
North-eastern	0.61	12.1	79.3	6.9	Best preserved

The table presents the average Velocity Ratio Index values and the corresponding classification of the quality of building materials for each façade of the Church of São João de Calvos. Quality of Building Materials percentages reflect the proportion of ashlars categorized as "Poor or very poor," "Fair," or "Good or very good," based on the comparison between in situ ultrasonic pulse velocity and reference values from fresh quarry specimens. Data by authors.

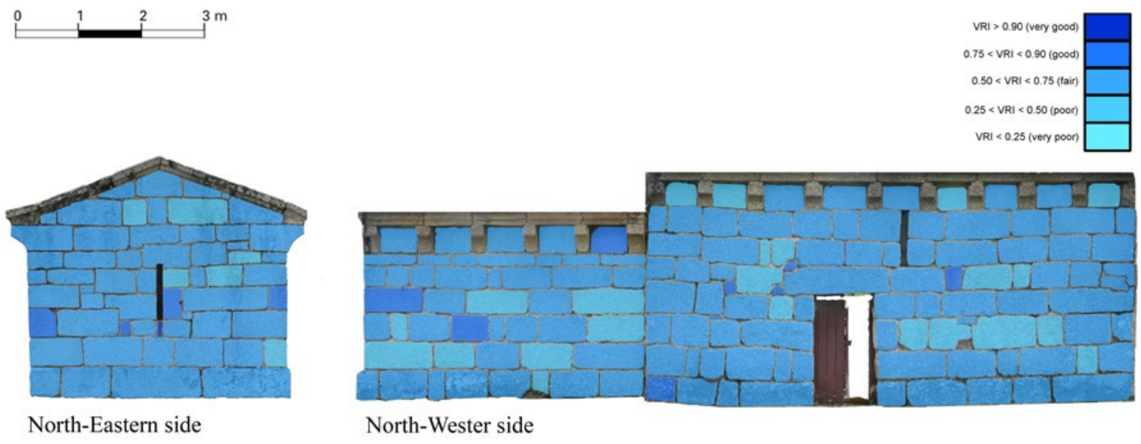

Figure 12. Results of the QMB characterisation across the north-eastern and north-western side of the church. Digital processing by authors.

5.3. Digitalisation

An important aspect of the building's digitization involved the production of detailed micro-photogrammetric models over areas of approximately 100 cm^2. This approach aimed to document the masonry to quantify material loss. The same method was used for monitoring the opening and evolution of fractures detected in the monument, specifically the crack in the lintel of the south-western façade caused by the structural load of the bell tower (Fig. 13a, b).

In the case of the lintel crack, differential micro-photogrammetry was preferred over traditional contact-based techniques, such as extensometers. While they provide accurate point measurements, require the installation of physical devices on the monument. In contrast, the proposed method is entirely non-invasive, preserves the aesthetic integrity of the structure, and allows for the simultaneous monitoring of fracture evolution and surface material loss over wider areas. Moreover, the absence of permanently installed sensors mitigates issues related to maintenance, potential vandalism, or theft, which are common in exposed heritage contexts.

The digitalization strategy adopted in this study combines non-contact diagnostic techniques with Heritage Building Information Modelling to support long-term monitoring within a 3D framework. To carry out these surveys, micro-photogrammetric reconstruction of selected areas should be repeated at one-year intervals, allowing for comparison between the initial survey (t0) and subsequent acquisitions (tn, Fig. 13c, d, e).

By monitoring volume loss and, consequently, material mass loss, this integrated approach across all façades could enable an overall estimation of the monument's annual mass loss due to stone decohesion. This procedure is defined as a differential micro-photogrammetric survey. Based on this method, the following equation (referring, for example, to the coarse-grained granitoid) can be formulated:

$$\Delta Vt_a = \Delta Vs_a \times (At/As) \qquad \text{[equation 2]}$$

Where:

ΔVt_a = total volume loss in the monument in one year (cm^3)

ΔVs_a = volume lost in the sample area in one year (cm^3)

As = reference area of 100 cm^2

At = total area of the monument's wall interested by coarse-grained granitoid (cm^2)

Consequently, the mass lost in one year (ΔMt_a in g) is calculated by the volume and the bulk density (ρ_B) of the selected stone (2.57 g/cm^3), considering the data in Table 1.

$\Delta Mt_a = \Delta Vt_a \times \rho_B$ [equation 3]

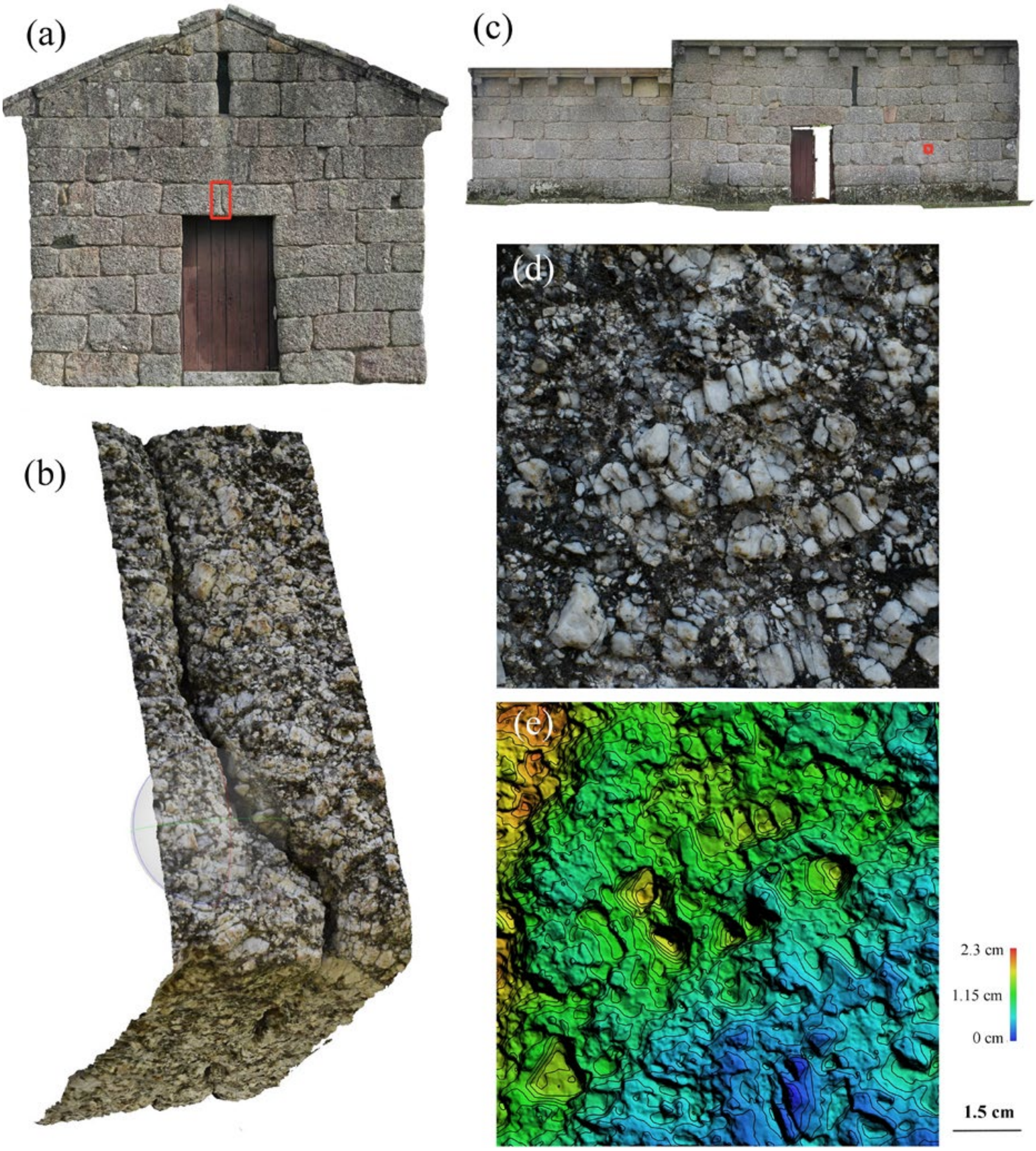

Figure 13. Micro-photogrammetry survey: (a, b) lesion affecting the architrave on the south-western façade, (c) scanned area by micro-photogrammetry on the north-western side of the church, (d) snapshot of the scanned area, (e) model of the 100 cm^2 scanned area, contour line spacing = 0.001 m. Digital processing by authors.

The proposed method for estimating annual material loss follows established principles used in geomorphology and stone-weathering research, particularly the Digital Elevation Model (DEM) differencing applied to highresolution image-based reconstructions. The calculation is not intended as an exact quantification of yearly erosion but as a first-order, scalable approximation that enables integration of surface-change data into HBIM. By repeating microphotogrammetric surveys over a fixed reference area, surface recession can be measured with submillimetric precision and subsequently extrapolated to the total surface area of the same lithology (At). Volume loss is then converted into mass using the bulk density of the relevant stone. This approach aligns with quantitative workflows in built-heritage diagnostics, which rely on multi-temporal 3D surveys to model micro-scale erosion over time (Galantucci and Fatiguso, 2019; Kong and Hucks., 2023; Mohan and Poobal, 2018).

To reinforce the methodological transparency of this approach, the manuscript distinguishes between the diagnostic capability of the technique, including its ability to detect minute surface variations and its role as an indicative metric for supporting preventive conservation strategies at monument and route scale. Although simpler physical instruments can complement the monitoring of the crack aperture, the non-contact, surface-based micro-photogrammetric method provides a richer dataset, better suited to the broader objectives of deterioration mapping, HBIM integration, and the development of a replicable monitoring protocol for the Romanesque Route.

Additionally, the photogrammetric survey planned within the monitoring programme would enable the evaluation of the extent of rock disintegration and the definition of a safety threshold. If this is exceeded, intervention through the application of water-repellent or consolidating products would become necessary. Continued surveys after treatment could also provide an effective means of assessing the performance of the applied products.

5.4. Heritage-Building Information Modelling

The dense point cloud generated from photogrammetric processing was exported in PLY format and imported into the modelling environment (VisualARQ/Rhino). This enabled direct modelling of the chapel geometry without requiring prior point cloud subsampling. Architectural elements were modelled interactively using a combination of parametric BIM objects, NURBS geometries, and custom parametric components implemented through Grasshopper, following an approach similar to that proposed by (Sun *et al.*, 2019). The resulting Level of Detail 200 HBIM model was exported to IFC, with semantic overlay generation and thematic mapping subsequently conducted in BonsaiBIM, as described in section 4.4 (Fig. 14).

The proposed texture-based semantic overlay methodology enabled independent annotation of heterogeneous analytical datasets without requiring permanent geometric subdivision of the architectural model. After establishing UV coordinates for the proxy geometries and exporting the corresponding unwrapped texture maps, updates to thematic information could be performed directly through modification of the associated 2D raster maps. Adding new thematic layers was done successfully by generating additional proxy geometries and their corresponding texture maps without requiring remodelling of the primary HBIM elements. Fig. 15 shows the stratigraphic units and the construction phases of the south-western and south-eastern facades added at a later stage.

Interoperability testing demonstrated that UV coordinates and texture references were correctly stored in IFC using IfcTriangulatedFaceSet, IfcIndexedTriangleTextureMap, IfcTextureVertexList, and IfcImageTexture entities. However, visualization and reconstruction of UV-mapped textures remained inconsistent across IFC software platforms. Tests conducted using BonsaiBIM, OpenIFC Viewer, and KITModelViewer showed that, although texture references and UV coordinate data persisted within the IFC schema, OpenIFC Viewer and BonsaiBIM failed to automatically reconstruct the UV mappings after reopening the model. KITModelViewer generates procedural UV coordinates ignoring or replacing those stored in the IFC file (Fig. 16). Additional scripting workflows using ifcopenshell were therefore required to rebuild UV layers from IFC file and preview materials within Blender after reopening the files.

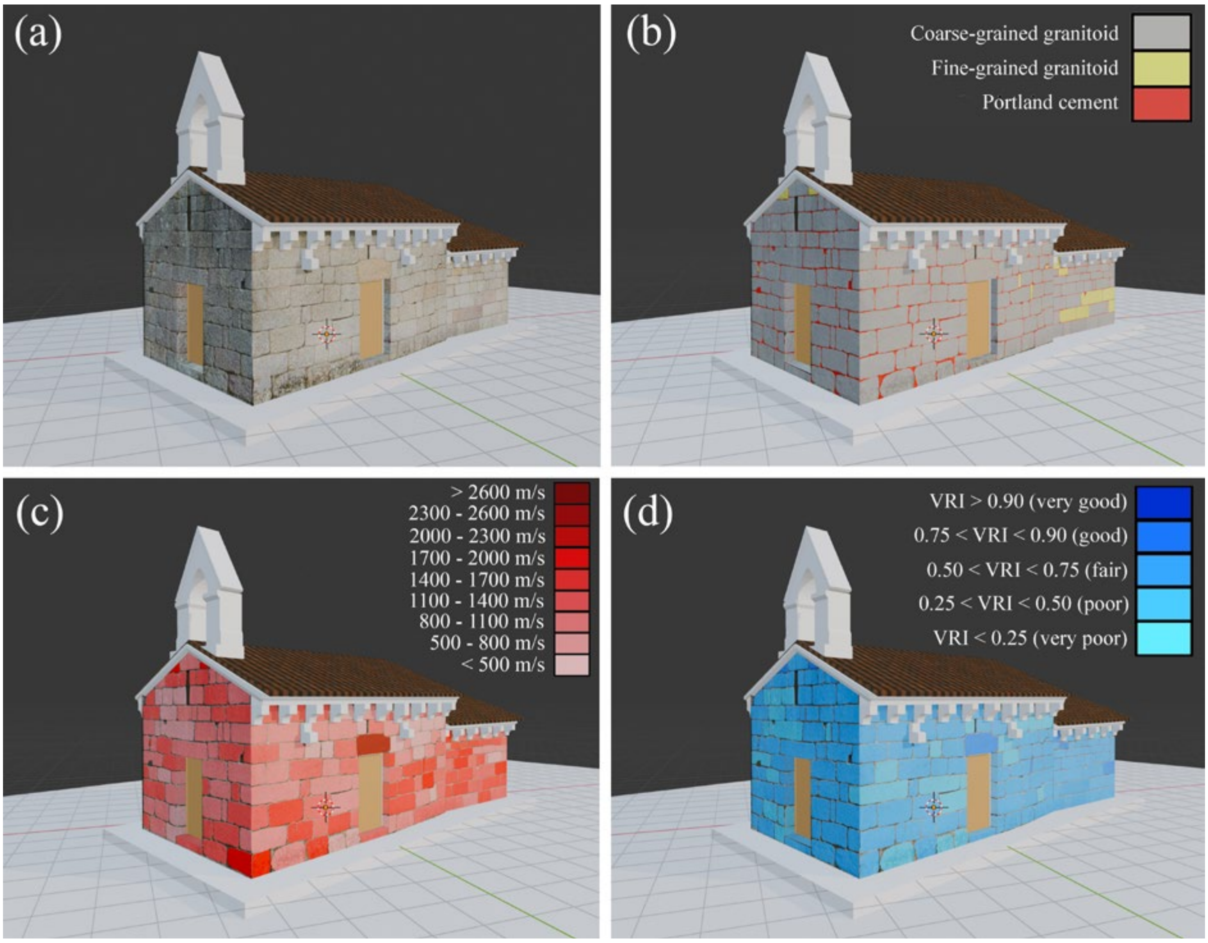

Figure 14. Digitalisation of the monument in a Building Information Modelling environment and related thematic maps. RGB texture (a), lithological features (b), ultrasonic characterisation (c), Velocity Ratio Index and quality of building materials data based on ultrasonic survey (d). Digital processing by authors.

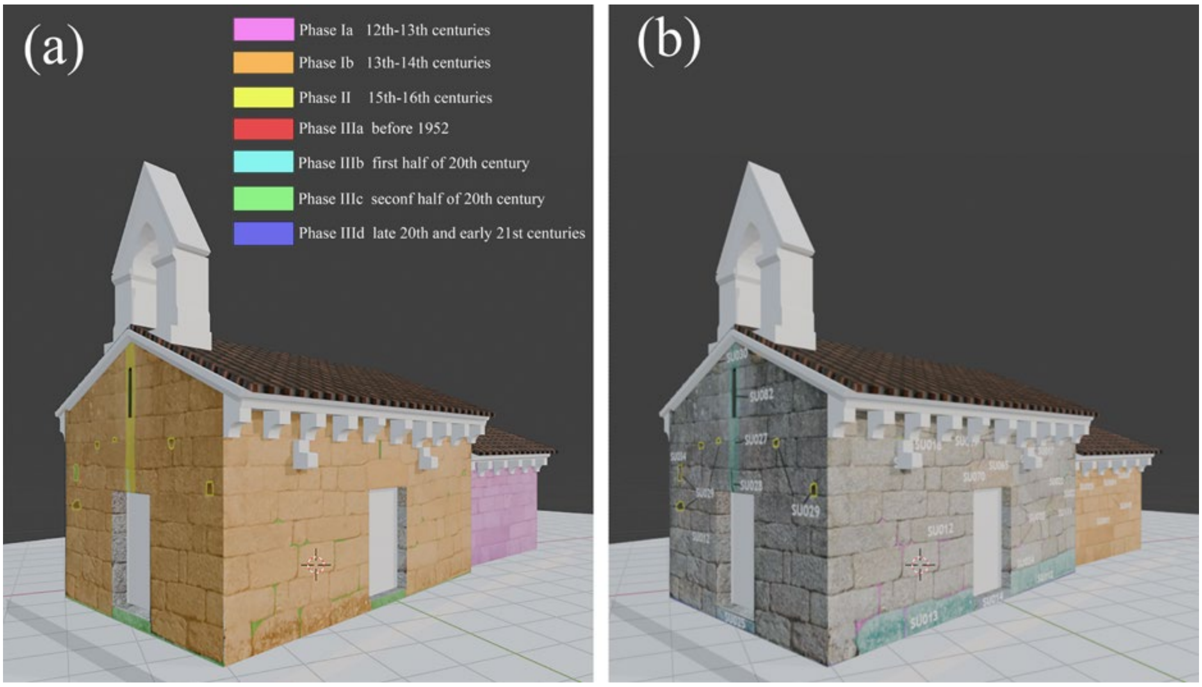

Figure 15. View of the south-western and south-eastern facades showing added thematic maps of construction phases (a) and stratigraphic units (b). Digital processing by authors.

Figure 16. South-western façade with incorrectly mapped texture in KitModelViewer.

Two strategies for enabling selective viewing of the thematic layers within an HBIM environment were explored. The first involved assigning proxy objects belonging to the same thematic category to dedicated IfcSpace entities. In this approach, all proxies associated with a specific analytical domain, such as building material quality mapping (QBM), were grouped within corresponding virtual semantic containers (e.g., IfcSpace/ThematicMap_QBM). The second strategy involves creating ifcGroup entities to organize thematic overlays. In this approach, a group collects all proxies belonging to a specific thematic category (e.g., IfcGroup/ThematicMap_QBM) and the remaining elements that do not have thematic overlays. This enabled the creation of complete thematic "views" in which analytical proxy layers could be visualized simultaneously with the remaining architectural context of the chapel.

The first strategy is semantically ambiguous since ifcSpace is conventionally intended to represent spatial or functional subdivisions of the building rather than analytical visualization layers. Conversely, the second strategy provides greater semantic consistency with the IFC schema, further supporting arbitrary logical associations without implying spatial or topological relations.

Nevertheless, interoperability testing revealed that support for selective visualization mechanisms remained heterogeneous across IFC software platforms, with ifcSpace showing wide support across the tested model viewers, and ifcGroup either unavailable (e.g. in OpenIFCViewer) or with less control over visualization than ifcSpace.

6. DISCUSSION

The integration of two-dimensional geological, historical-archaeological, ultrasonic, and building material quality maps onto three-dimensional representations of monuments constitutes a strategic approach for the diagnosis, conservation, and enhancement of cultural heritage.

This methodology overcomes the reading limitations of traditional 2D surveys by offering an intuitive, three-dimensional representation of the condition of the structure. Integrating diagnostic data directly onto the real geometry of the artifact makes it possible to precisely identify risk areas, visualize discontinuities, cracks, or hidden deterioration, and facilitate the planning of restoration interventions. The proposed workflow demonstrates that heterogeneous analytical datasets can be integrated within an HBIM environment without requiring permanent geometric subdivision of the architectural model. This avoids the combinatorial increase in model complexity typically associated with geometry-driven semantic partitioning approaches.

The proposed methodology prioritizes lightweight semantic visualization and interdisciplinary annotation over object-level semantic decomposition. Consequently, thematic information encoded exclusively within texture masks remains primarily visual unless accompanied by external metadata structures or additional semantic indexing mechanisms. Thus, in this framework the semantic interpretation emerges from the combination of IFC metadata structures, visual overlays and grouping relationships.

From a methodological perspective, the proposed workflow combines surveying techniques (such as laser scanning or photogrammetry) non-destructive diagnostic techniques, and IFC-based semantic modelling creating an informative digital model that can be constantly updated over time.

Because the methodology is independent of the subdivision, other heterogenous thematic maps can be incrementally added, including degradation maps, thermographic surveys, humidity maps (Solla *et al.*, 2020) and other non-destructive mechanical data such as rebound tests to assess compressive strength and homogeneity.

Moreover, these hybrid models provide an ideal basis for structural simulations, predictive analyses, or augmented and virtual reality applications, including the construction phases, thus making communication more effective between professionals, heritage authorities, and the public.

In a context where heritage conservation increasingly demands precise and sustainable solutions, the combined use of 2D diagnostic maps on 3D models stands out as an essential tool for the informed and scientific management of monumental assets.

The current approach is effective for any type of analysis that is surface based, such as degradation. Although intersection and overlapping of proxy geometries may produce unused areas in their respective UV maps, it does not introduce spatial and semantic ambiguities. Conversely, this methodology becomes less effective with volumetric analyses where the derived semantic information pertains to elements of different depths.

An alternative approach to the currently proposed methodology could involve assigning multiple thematic textures to a single architectural object, thus overcoming the need for overlapping proxy geometries. Although IFC supports the assignment of multiple textures through IfcSurfaceStyleWithTextures, the standard does not define how these textures should be interactively visualized or selectively controlled within viewing applications. Consequently, the interpretation and presentation of texture layers is delegated to software implementations such as KITModelViewer. Arguably, IfcSurfaceStyleWithTextures was not designed to support multiple independently viewable analytical textures. Yet, due to the abstract nature of IFC, this is a possible approach that may be implemented as a plugin for a viewer to support the specific needs of the Cultural Heritage field. Future work should investigate the development of custom IFC viewer extensions or shader-based visualization systems capable of interactively managing multiple analytical texture layers within HBIM environments.

Another potential development of the proposed methodology involves complementing the visual texture overlays with categorical semantic indexing structures. In this scenario, thematic maps would continue to operate as lightweight visual representations, while individual color ranges or texture regions could be associated with semantic classes, metadata tables, or external classification structures. Such an approach could partially address the querying limitations of raster-based semantic representations without requiring exhaustive geometric subdivision of the architectural model. Future work should evaluate mechanisms for linking texture-based classifications with IFC property structures or external semantic databases.

7. CONCLUSIONS

This study establishes a replicable multidisciplinary protocol for the documentation, diagnosis, and monitoring of architectural heritage, using the Church of São João de Calvos as a pilot case. By combining archaeological stratigraphy, petrographic analysis, and non-destructive testing (NDT) within a Heritage Building Information Modelling (HBIM) framework, the research moves beyond static 2D documentation toward a dynamic, data-driven tool for preventive conservation.

The stratigraphic analysis of the elevations allowed for the identification of a complex "building biography" characterised by three main phases. The results redefine the church's chronology, revealing that the medieval structures previously considered Late Romanesque actually correspond to two distinct moments between the 12th and 13th centuries. This evolution, from a modest rural temple to a Gothic-influenced nave, followed by modern interventions, demonstrates that HBIM can effectively spatialize historical narratives, making them accessible for both scientific research and cultural-tourism itineraries like the *Rota do Românico*.

A central outcome of this research is the definition of a standardized diagnostic protocol designed to be adopted by heritage managers. The methodology consists of four integrated phases:

1. Multi-source Survey: High-resolution 3D capture paired with stratigraphic analysis to establish the geometric and historical baseline
2. Material Diagnosis: Use of Velocity Ratio Indices (VRI) to quantify stone degradation and correlate it with environmental exposure
3. Semantic HBIM Integration: The use of texture-based overlays to visualize analytical datasets (e.g. ultrasonic) without compromising the model's computational lightness
4. Continuous Monitoring: The implementation of Differential Photogrammetric Surveys to track structural pathologies (such as the lintel crack) and quantify annual material loss with sub-millimetric precision

The integration of these diagnostic layers into an OpenBIM environment ensures interoperability and long-term data persistence. The study demonstrates that this approach is particularly effective for surface-based degradation, providing a scalable model for the sustainable management of monumental assets. While traditional sensors (extensometers) remain valid for point measurements, the proposed non-contact digital workflow offers a richer, more comprehensive dataset for large-scale preventive strategies.

Furthermore, while this study focuses on the pilot case of São João de Calvos, the methodology is designed to be scalable to the entire 'Route of the Romanesque'. The transition from a single-site HBIM to a territorial-scale digital system is facilitated by the adoption of a standardized semantic protocol, which ensures data harmonization across diverse assets. By utilizing a common lexicon for material decay and stratigraphic units, the proposed framework allows for the creation of a multi-asset digital repository. This system can serve as a centralized Decision Support System (DSS), enabling regional authorities to implement long-term monitoring and prioritize conservation efforts based on objective, cross-comparable data. Consequently, this research establishes the groundwork for a distributed digital management model, transforming individual heritage records into a cohesive territorial management tool.

Supplementary information ↑

Funding sources

The authors gratefully acknowledge the IN2PAST "Laboratório Associado para a Investigação e Inovação em Património, Artes, Sustentabilidade e Território" for funding the project "The Romanesque-style rural church of Portugal: An initial stride towards the complete digitalization by Heritage-BIM. The case study of S. João de Calvos (Guimarães, 13th Cent. AD)." Project code: EXPL/In2Past/2024/12

Fabio Sitzia gratefully acknowledge the European Union – Portuguese Recovery and Resilience Plan, Grant Contract number: Sustainable Stone by Portugal, Call: 2021- C05i0101-02—agendas/alianças mobilizadoras para a reindustrializaçã̃o – PRR, Proposal: C632482988-00467016.

Supplementary material

This article includes two supplementary files available on the journal's website:

Annex SF1: Periodized table of stratigraphic units, Church of São João de Calvos (Guimarães). Recorder: research team.

Annex SF2: Stratigraphic diagram representing the building's sequence. Digital processing by authors.

Data availability

The data that support the findings of this study are available from the corresponding author Fabio Sitzia, upon reasonable request.

Acknowledgements

Not applicable.

Authorship contribution statement

Fabio Sitzia: project administration, conceptualization, data curation, formal analysis, investigation, resources, software exploitation, supervision, methodology, validation, visualization, writing—original draft, writing—review and editing.

Filipe Brandão: conceptualization, data curation, formal analysis, investigation, resources, software exploitation, supervision, methodology, validation, visualization, writing—original draft, writing—review and editing.

Paulo Bernardes: conceptualization, data curation, formal analysis, investigation, resources, software exploitation, supervision, methodology, validation, visualization, writing—original draft, writing—review and editing.

Vera Pires: conceptualization, data curation, formal analysis, investigation, resources, software exploitation, supervision, methodology, validation, visualization, writing—original draft, writing—review and editing.

Rebeca Blanco Rotea: conceptualization, data curation, formal analysis, investigation, resources, software exploitation, supervision, methodology, validation, visualization, writing—original draft, writing—review and editing.

Jorge Ribeiro: project administration, conceptualization, data curation, formal analysis, investigation, resources, software exploitation, supervision, methodology, validation, visualization, writing—original draft, writing—review and editing.

All authors have read and agreed to the published version of the manuscript.

Competing interests

The authors declare that they have no known competing financial interests or personal relationships that could have appeared to influence the work reported in this paper.

Authors have conduct themselves with integrity, fidelity, and honesty. Authors will openly take responsibility for their actions and only make agreements which they intend to keep. Authors will not intentionally engage in or participate in any form of malicious harm to another person or animal.

Statement on the use of Artificial Intelligence

Not applicable.

REFERENCES

Azkarate Garai-Olaun, A. (2013). "La construcción y lo construido. Arqueología de la Arquitectura." In: Quirós Castillo, J. A. (Ed.). *La materialidad de la historia. La arqueología en los inicios del siglo XXI*. Madrid: Akal, pp. 281-308.

Azkarate Garai-Olaun, A., Caballero Zoreda, L., and Quirós Castillo, J. A. (2002). "Arqueología de la Arquitectura: definición disciplinar y nuevas perspectivas." *Arqueología de la Arquitectura*, 1, pp. 7-10. DOI: https://doi.org/10.3989/arqarqt.2002.i1

Bastem, S. S., and Cekmis, A. (2022). "Development of historic building information modelling: a systematic literature review." *Building Research & Information*, 50 (5), pp. 527-558. DOI: https://doi.org/10.1080/09613218.2021.1983754

Blanco-Rotea, R. (2017). "Arquitectura y paisaje. Aproximaciones desde la arqueología." *Arqueologia de la Arquitectura,* 14, e051. DOI: https://doi.org/10.3989/arq.arqt.2017.007

Borkowski, A. S., and Kubrat, A. (2024). "Integration of Laser Scanning, Digital Photogrammetry and BIM Technology: A Review and Case Studies." *Eng*, 5 (4), pp. 2395-2409. DOI: https://doi.org/10.3390/eng5040125

Brusaporci, S., Trizio, I., Ruggeri, G., Maiezza, P., Tata, A., and Giannangeli, A. (2018). "AHBIM per l'analisi stratigrafica dell'architettura storica." *Restauro Archeologico*, 26 (1), pp. 112-131. DOI: https://doi.org/10.13128/RA-23463

Caballero Zoreda, L. (1995). "Método para el análisis estratigráfico de construcciones históricas o 'lectura de paramentos'." *Informes de la Construcción*, 46 (435), pp. 37-46. DOI: https://doi.org/10.3989/ic.1995.v46.i435.1096

Casula, G., Fais, S., Bianchi, M. G., and Ligas, P. (2026). "A Multi-Disciplinary Approach to the Identification and Characterisation of Areas of Potential Damage in the Building Materials of Ancient Monuments." *Sensors*, 26 (5), 1648. DOI: https://doi.org/10.3390/s26051648

Casula, G., Fais, S., Cuccuru, F., Bianchi, M. G., and Ligas, P. (2024). "An Integrated Petrographic, Geomatic and Geophysical Approach for the Characterisation of the Carbonate Rocks of the Calcari di Cagliari Formation." *Minerals*, 14 (5), 501. DOI: https://doi.org/10.3390/min14050501

Charef, R., Emmitt, S., Alaka, H., and Fouchal, F. (2019). "Building Information Modelling adoption in the European Union: An overview." *Journal of Building Engineering*, 25, 100777. DOI: https://doi.org/10.1016/j.jobe.2019.100777

Chelaru, B., Onuțu, C., Ungureanu, G., and Șerbănoiu, A. A. (2024). "Integration of point cloud, historical records, and condition assessment data in HBIM." *Automation in Construction*, 161, 105347. DOI: https://doi.org/10.1016/J.AUTCON.2024.105347

Chiabrando, F., Lo Turco, M., and Rinaudo, F. (2017). "Modeling the decay in an HBIM starting from 3d point clouds. A followed approach for cultural heritage knowledge." *The International Archives of the Photogrammetry, Remote Sensing and Spatial Information Sciences*, XLII-2/W5, pp. 605-612. DOI: https://doi.org/10.5194/isprs-archives-XLII-2-W5-605-2017

Colao, F., Fantoni, R., Ortiz, P., Vazquez, M. A., Martin, J. M., Ortiz, R., and Idris, N. (2010). "Quarry identification of historical building materials by means of laser induced breakdown spectroscopy, X-ray fluorescence and chemometric analysis." *Spectrochimica Acta - Part B Atomic Spectroscopy*, 65 (8), pp. 688-694. DOI: https://doi.org/10.1016/j.sab.2010.05.005

Coll-Pla, S., López-Piquer, M., Lluis-Ginovart, J., and Costa-Jover, A. (2019). "Deformation Process of Romanesque Masonry Constructions: The Case of Vall d'Aran Churches." In: Aguilar, R., Torrealva, D., Moreira, S., Pando, M. A., and Ramos, L. F. (Eds.). *Structural Analysis of Historical Constructions*. RILEM Bookseries, 18. Cham: Springer. DOI: https://doi.org/10.1007/978-3-319-99441-3_7

Columbu, S., Palomba, M., Sitzia, F., Carcangiu, G., and Meloni, P. (2022). "Pyroclastic Stones as Building Materials in Medieval Romanesque Architecture of Sardinia (Italy): Chemical-Physical Features of Rocks and Associated Alterations." *International Journal of Architectural Heritage*, 16 (1), pp. 49–66. DOI: https://doi.org/10.1080/15583058.2020.1749729

Croce, V., Bevilacqua, M. G., Caroti, G., and Piemonte, A. (2021). "Connecting Geometry and Semantics via Artificial Intelligence: From 3d classification of Heritage Data to H-BIM representations." *The International Archives of the Photogrammetry, Remote Sensing and Spatial Information Sciences*, XLIII-B2-2, pp. 145–152. DOI: https://doi.org/10.5194/isprs-archives-XLIII-B2-2021-145-2021

Cuccuru, F., Fais, S., and Ligas, P. (2014). "Dynamic elastic characterisation of carbonate rocks used as building materials in the historical city centre of Cagliari (Italy)." *Quarterly Journal of Engineering Geology and Hydrogeology,* 47, pp. 259-266. DOI: https://doi.org/10.1144/qjegh2013-061

Czubla, P., Brykała, D., Dąbski, M., Gierszewski, P., Błaszkiewicz, M., Mosakowski, Z., and Lamparski, P. (2024). "Unobvious geoheritage in sacral buildings: millstones in churches of NE Poland from a geological and geomorphological perspective." *Geographia Polonica*, 97 (3), pp. 327-354. DOI: https://doi.org/10.7163/GPol.0282

Fais, S., Cuccuru, F., Ligas, P., Casula, G., and Bianchi, M. G. (2017). "Integrated ultrasonic, laser scanning and petrographical characterisation of carbonate building materials on an architectural structure of a historic building." *Bulletin of Engineering Geology and the Environment*, 76, pp. 71-84. DOI: https://doi.org/10.1007/s10064-015-0815-9

Fitz, D. V., and Saleeb, N. (2019). "Examining the quality and management of non-geometric building information modelling data at project hand-over." *Architectural Engineering and Design Management,* 15 (4), pp. 297-310. DOI: https://doi.org/10.1080/17452007.2018.1560243

Galantucci, R. A., and Fatiguso, F. (2019). "Advanced damage detection techniques in historical buildings using digital photogrammetry and 3D surface anlysis." *Journal of Cultural Heritage*, 36, pp. 51-62. DOI: https://doi.org/10.1016/j.culher.2018.09.014

Garagnani, S., Gaucci, A., and Gruška, B. (2016)." From the archaeological record to archaeobim: the case study of the Etruscan temple of Uni in Marzabotto." *Virtual Archaeology Review*, 7 (15), pp. 77-86. DOI: https://doi.org/10.4995/var.2016.5846

Godager, B., Mohn, K., Merschbrock, C., Klakegg, O. J., and Huang, L. (2022). "Towards an improved framework for Enterprise Bim: the Role of Iso 19650." *Journal of Information Technology in Constructionk¸* 27, pp. 1075-1103. DOI: https://doi.org/10.36680/j.itcon.2022.053

Górska-Zabielska, M. (2024). "Scandinavian Erratics in the Cultural Heritage Sites of Western Poland." *Land*, 13 (8), 1282. DOI: https://doi.org/10.3390/land13081282

Harris, E. (1989). *Principles of archaeological stratigraphy.* London: Academic Press, 2nd ed.

Hatır, M. E., Korkanç, M., and Başar, M. E. (2019). "Evaluating the deterioration effects of building stones using NDT: the Küçükköy Church, Cappadocia Region, central Turkey." *Bulletin of Engineering Geology and the Environment*, 78, pp. 3465-3478. DOI: https://doi.org/10.1007/s10064-018-1339-x

Kahraman, S., Ulker, U., and Delibalta, M. S. (2007). "A quality classification of building stones from P-wave velocity and its application to stone cutting with gang saws." *The Journal of the Southern African Institute of Mining and Metallurgy*, 107, pp. 427-430.

Karasaka, L., and Ulutas, N. (2023). "Point Cloud-Based Historical Building Information Modeling (H-BIM) in Urban Heritage Documentation Studies." *Sustainability*, 15 (13), 10726. DOI: https://doi.org/10.3390/su151310726

Kong, X., and Hucks, R. G. (2023). "Preserving our heritage: A photogrammetry-based digital twin framework for monitoring deteriorations of historic structures." *Automation in Construction*, 152, 104928. DOI: https://doi.org/10.1016/j.autcon.2023.104928

Lisci, C., Sitzia, F., Pires, V., Aniceto, M., and Mirão, J. (2023). "Stone Endurance: A Comparative Analysis of Natural and Artificial Weathering on Stone Longevity." *Heritage*, 6 (6), pp. 4593-4617. DOI: https://doi.org/10.3390/heritage6060244

Lisci, C., Sitzia, F., Pires, V., and Mirão, J. (2022). "Building stones durability by UVA radiation, moisture and spray accelerated weathering." *Journal of Building Pathology and Rehabilitation*, 7 (1), 60. DOI: https://doi.org/10.1007/s41024-022-00196-9

Lovell, L. J., Davies, R. J., and Hunt, D. V. L. (2023). "The Application of Historic Building Information Modelling (HBIM) to Cultural Heritage: A Review." *Heritage*, 6 (10), pp. 6691-6717. DOI: https://doi.org/10.3390/heritage6100350

Mammoli, R., Mariotti, C., and Quattrini, R. (2021). "Modeling the Fourth Dimension of Architectural Heritage: Enabling Processes for a Sustainable Conservation." *Sustainability*, 13 (9), 5173. DOI: https://doi.org/10.3390/su13095173

Mohan, A., and Poobal, S. (2018). "Crack detection using image processing: A critical review and analysis." *Alexandria Engineering Journal*, 57 (2), pp. 787-798. DOI: https://doi.org/10.1016/j.aej.2017.01.020

Nguyen, T. D., and Adhikari, S. (2023). "The Role of BIM in Integrating Digital Twin in Building Construction: A Literature Review." *Sustainability*, 15 (13), 10462. DOI: https://doi.org/10.3390/su151310462

Nieto-Julián, E., Robador, M. D., Moyano, J., and Bruno, S. (2025). "Semantic HBIM for Heritage Conservation: A Methodology for Mapping Deterioration and Structural Deformation in Historic Envelopes." *Buildings*, 15 (12), 1990. DOI: https://doi.org/10.3390/buildings15121990

Over, J.-S. R., Ritchie, A. C., Kranenburg, Ch. J., Brown, J. A., Buscombe, D. D., Noble, T., Sherwood, Ch. R., Warrick, J. A., and Wernette, Ph. A. (2021). *Processing Coastal Imagery with Agisoft Metashape Professional Edition, Version 1.6—Structure from Motion Workflow Documentation*. Open-File Report 2021-1039. DOI: https://doi.org/10.3133/ofr20211039

Pan, X., Mateen Khan, A., Eldin, S. M., Aslam, F., Kashif Ur Rehman, S., and Jameel, M. (2024). "BIM adoption in sustainability, energy modelling and implementing using ISO 19650: A review." *Ain Shams Engineering Journal*, 15 (1), 102252. DOI: https://doi.org/10.1016/j.asej.2023.102252

Pina, L. de (1952). "O Românico no Concelho de Guimarães." *Revista de Guimarães*, 62 (1-2), pp. 119-132.

Pucci, M. (2014). "Photogrammetry of the Microcosms: Investigating the landscape of single stones to create bases of knowledge." In: Boerner, W. (Ed.). *19th International Conference on Cultural Heritage and New Technologies*. Wien: Museen der Stadt Wien – Stadtarchäologie.

Puerto, A., Castañeda, K., Sánchez, O., Peña, C. A., Gutiérrez, L., and Sáenz, P. (2024). "Building information modeling and complementary technologies in heritage buildings: A bibliometric analysis." *Results in Engineering*, 22, 102192. DOI: https://doi.org/10.1016/J.RINENG.2024.102192

Rosa, J., Moreira, N., Santos, J., and Ribeiro, S. (2023). "Trigaches Marbles (São Brissos, Beja, Portugal): petrographic and geochemical characterisation of a historical dimension stone." In: *VII Global Stone Congress*. Évora: Universidade de Évora, 115.

Rudolph, C. (2019). *A Companion to Medieval Art: Romanesque and Gothic in Northern Europe*. Hoboken: Wiley. DOI: https://doi.org/10.1002/9781119077756

Santoni, A., Martín-Talaverano, R., Quattrini, R., and Murillo-Fragero, J. I. (2021). "HBIM approach to implement the historical and constructive knowledge. The case of the Real Colegiata of San Isidoro (León, Spain)." *Virtual Archaeology Review*, 12 (24), pp. 49-65. DOI: https://doi.org/10.4995/var.2021.13661

Sitzia, F. (2024). "The Unesco 14th Century Fortifications of Cerca Nova (Évora, Portugal): Provenience and Classification of Geo-Materials and Vascular Plants Inventory." *Estudos do Quaternário / Quaternary Studies*, 24, pp. 24-33. DOI: https://doi.org/10.30893/eq.v0i24.220

Solla, M., Gonçalves, L. M. S., Gonçalves, G., Francisco, C., Puente, I., Providência, P., Gaspar, F., and Rodrigues, H. (2020). "A Building Information Modeling Approach to Integrate Geomatic Data for the Documentation and Preservation of Cultural Heritage." *Remote Sensing*, 12 (24), 4028. DOI: https://doi.org/10.3390/rs12244028

Stück, H., Siegesmund, S., and Rüdrich, J. (2011). "Weathering behaviour and construction suitability of dimension stones from the Drei Gleichen area (Thuringia, Germany)." *Environmental Earth Sciences*, 63, 00. 1763-1786.. DOI: https://doi.org/10.1007/s12665-011-1043-7

Sun, Z., Xie, J., Zhang, Y., and Cao, Y. (2019). "As-Built BIM for a Fifteenth-Century Chinese Brick Structure at Various LoDs." *ISPRS International Journal of Geo-Information*, 8 (12), 577. DOI: https://doi.org/10.3390/ijgi8120577

Volk, R., Stengel, J., and Schultmann, F. (2014). "Building Information Modeling (BIM) for existing buildings - Literature review and future needs." *Automation in Construction*, 38, pp. 109-127. DOI: https://doi.org/10.1016/j.autcon.2013.10.023

Wang, Q., and Kim, M. K. (2019). "Applications of 3D point cloud data in the construction industry: A fifteen-year review from 2004 to 2018." *Advanced Engineering Informatics*, 39, pp. 306-319. DOI: https://doi.org/10.1016/J.AEI.2019.02.007